the plant journal

SEB SOCIETY FOR EXPERIMENTAL BIOLOGY

The Plant Journal (2020) doi: 10.1111/tpj.14704

Characterization of an alkylresorcinol synthase that forms phenolics accumulating in the cuticular wax on various organs of rye (*Secale cereale*)

Yulin Sun[1,†], Ruonan Yao[1,†], Xiufeng Ji[2], Hongqi Wu[3], Alvaro Luna[1], Zhonghua Wang[3] and Reinhard Jetter[1,2,*]

[1]*Department of Botany, University of British Columbia, 6270 University Blvd., Vancouver V6T 1Z4, Canada,*

[2]*Department of Chemistry, University of British Columbia, 2036 Main Mall, Vancouver V6T 1Z1, Canada, and*

[3]*State Key Laboratory of Crop Stress Biology in Arid Areas, College of Agronomy, Northwest A&F University, Yangling, Shaanxi 712100, China*

Received 3 September 2019; revised 18 December 2019; accepted 7 January 2020.

*For correspondence (e-mail reinhard.jetter@botany.ubc.ca).

†These authors contributed equally to this work and should be considered joint first authors.

SUMMARY

Alkylresorcinols are bioactive compounds produced in diverse plant species, with chemical structures combining an aliphatic hydrocarbon chain and an aromatic ring with characteristic hydroxyl substituents. Here, we aimed to isolate and characterize the enzyme that forms the alkylresorcinols accumulating in the cuticular wax on the surface of all above-ground organs of rye. Based on sequence homology with other type-III polyketide synthases, a candidate alkylresorcinol synthase was cloned. Yeast heterologous expression showed that the enzyme, ScARS, is highly specific for the formation of the aromatic resorcinol ring structure, through aldol condensation analogous to stilbene synthases. The enzyme accepts long-chain and very-long-chain acyl-CoA starter substrates, preferring saturated over unsaturated chains. It typically carries out three rounds of condensation with malonyl-CoA prior to cyclization, with only very minor activity for a fourth round of malonyl-CoA condensation and cyclization to 5-(2′-oxo)-alkylresorcinols or 5-(2′-hydroxy)-alkylresorcinols. Like other enzymes involved in cuticle formation, ScARS is localized to the endoplasmic reticulum. *ScARS* expression patterns were found correlated with alkylresorcinol accumulation during leaf development and across different rye organs. Overall, our results thus suggest that ScARS synthesizes the cuticular alkylresorcinols found on diverse rye organ surfaces.

Keywords: biosynthesis, chain lengths, cuticular wax, fatty acids, phenolics, polyketide synthase.

INTRODUCTION

The primary above-ground surfaces of vascular plants are coated by a cuticle, a thin layer of lipophilic compounds that acts as a protective barrier against the environment. In particular, plant cuticles minimize non-stomatal transpiration, reduce the adhesion of pathogen spores and dust, protect tissues from UV radiation, mediate interactions with microbes as well as insects, and prevent deleterious fusions between plant organs (Riederer and Müller, 2007). Plant cuticles consist of the organic-solvent-insoluble fatty acid polyester cutin (Fich *et al.*, 2016) and organic-solvent-soluble cuticular waxes (Yeats and Rose, 2013). The latter are typically mixtures of saturated very-long-chain fatty acid (VLCFA) derivatives, that is, unbranched aliphatic compounds with 20 or more carbon atoms (Samuels *et al.*, 2008). Compounds vary by functional groups, and acids, aldehydes, primary alcohols and alkanes are typically found in plant cuticular waxes (Busta and Jetter, 2018). The chain lengths within these compound classes range from C_{24} to C_{40}, with C_{26}–C_{32} homologs prevailing in most cases. Fatty acids and wax alcohols are also found combined in esters with chain lengths C_{38}–C_{70} (Lai *et al.*, 2007). The absolute amounts of waxes and their relative composition both vary greatly between different plant species, between organs and between developmental stages of the same organ (Jetter and Schäffer, 2001).

Our understanding of the processes underlying the formation of cuticular waxes has greatly improved over past decades, mainly through molecular genetic work on Arabidopsis. There, the broad array of wax compounds is formed by dedicated pathways comprising three major stages, first recruiting substrates from fatty acid *de novo* biosynthesis, then elongating their hydrocarbon backbones, and finally elaborating their functional groups

© 2020 The Authors.
The Plant Journal © 2020 John Wiley & Sons Ltd

(Li-Beisson *et al.*, 2013; Hegebarth and Jetter, 2017). Initially, the C_{16}/C_{18} acyl-ACPs formed by plastidial elongation complexes are hydrolyzed (Dörmann *et al.*, 2000), exported from the plastid, transferred to the endoplasmic reticulum (ER), and re-activated into acyl-CoAs (Bernard and Joubes, 2013; Li-Beisson *et al.*, 2013). En route to wax formation, the C_{16}/C_{18} acyl-CoAs are then elongated in reaction cycles catalyzed by fatty acid elongation (FAE) complexes, each adding two carbons to the growing hydrocarbon chain (Haslam and Kunst, 2013). One of the FAE enzymes, the ketoacyl-CoA synthetase (KCS), first condenses the acyl-CoA substrate with one malonate extender, to generate a hydrocarbon chain two carbons longer than in the substrate acyl chain. Then, the other three enzymes (two reductases and a dehydratase) reduce the resulting keto group into a methylene unit, thus converting a β-ketoacyl intermediate into the elongated acyl (Samuels *et al.*, 2008). The resulting acyl-CoAs are then, in the final stage of wax biosynthesis, converted into corresponding aldehydes and alcohols, thereby retaining the hydrocarbon backbones and thus leading to products with mainly even numbers of carbons (Rowland *et al.*, 2006). Alternatively, the head group can be cleaved off to generate alkanes with one carbon less, and thus predominantly odd numbers of carbons (Bernard *et al.*, 2012).

In addition to the VLCFA derivatives, cuticular waxes of many plant species also contain aromatic and alicyclic compounds (Jetter *et al.*, 2007). Aromatics have been reported as wax constituents mainly in the form of phenylpropanoids and alkylresorcinols (Gülz *et al.*, 1992; Jetter *et al.*, 2002; Ji and Jetter, 2008). The latter have been found as natural products in diverse species especially in the Poaceae, in many cases from plant tissue at or near the surface (Suzuki *et al.*, 1999; Deszcz and Kozubek, 2000; Ross *et al.*, 2001, 2003; Zarnowski and Suzuki, 2004; Andersson *et al.*, 2008; Kulawinek and Kozubek, 2008; Landberg *et al.*, 2008; Wang *et al.*, 2019), suggesting that they may accumulate in the cuticular wax mixtures coating respective organs in all these species. For rye (*Secale cereale* L.), the leaf alkylresorcinols were indeed localized to the cuticular wax rather than the interior parts of the tissue (Ji and Jetter, 2008). However, it is currently not clear how the presence of alkylresorcinols affects cuticle properties, and which biological functions they might have. In order to gain insights into cuticular alkylresorcinol biology, an improved biochemical understanding of the mechanisms leading to their formation is necessary, and corresponding genes must be cloned from appropriate plant species and tissues.

To date, no enzymes involved in the formation of the very-long-chain cuticular alkylresorcinols have been described. However, a few enzymes with alkylresorcinol synthase (ARS) activity forming alkylresorcinols with shorter side chains, in other biological contexts, were characterized both from bacterial and plant species. Early on, two ARSs were shown to be involved in the formation of sorgoleone, a resorcinolic secondary metabolite with an unsaturated C_{15} alkyl side chain found in the root exudate of *Sorghum bicolor* (Cook *et al.*, 2010). Three ARSs from rice, *Oryza sativa*, were found to have very similar primary structures and function, likely forming root phytoanticipins (Matsuzawa *et al.*, 2010). Besides these monocot enzymes, very few ARSs have been reported from other plant lineages, most notably including a tetraketide synthase from *Cannabis sativa* involved in forming olivetol and Δ9-tetrahydrocannabinol precursors with C_5 side chains (Gagne *et al.*, 2012). An ARS from *Physcomitrella patens* was found to form mainly 2′-oxo-derivatives with side chain lengths varying widely from C_5 to C_{23}, but corresponding compounds could not be detected in moss extracts (Kim *et al.*, 2013; Li *et al.*, 2018), even though mutant analyses suggested cuticle localization (Li *et al.*, 2018). Similar ARSs have been described from filamentous fungi, including *Neurospora crassa*, where they produce mixed products including alkylresorcylic acid, alkylresorcinols and alkylpyrones (Funa *et al.*, 2007). Finally, several ARSs have also been described from bacteria, most prominently the enzyme responsible for forming the resorcinolic structures with C_9–C_{21} side chains found in *Azotobacter vinelandii* cysts (Funa *et al.*, 2006).

Plant ARSs are members of the type-III polyketide synthase (PKS) family of proteins, a large group of enzymes that produce a wide array of secondary metabolites. In general, PKSs first bind a starter substrate, before catalyzing its iterative condensations with multiple malonyl-CoA units and a final, intramolecular cyclization (Austin and Noel, 2003; Abe and Morita, 2010). The latter cyclization may proceed through C-6 → C-1 Claisen condensation, leading to phloroglucinolic structures, as in the very well-studied chalcone synthase (CHS) enzymes crucial for flavonoid biosynthesis in all plant species (Figure 1a). Alternatively, C-2 → C-7 aldol condensation may lead to resorcinolic ring structures, as in the stilbene synthase (STS) enzymes found in some species (Figure 1b; Austin *et al.*, 2004). Both CHS-type and STS-type PKS enzymes use *p*-coumaroyl-CoA as starter substrate, and thus they rely exclusively on aromatic building blocks to which they add a second aromatic ring structure. In contrast, ARSs must utilize aliphatic starters, most likely acyl-CoAs derived from fatty acids of various chain lengths, for specific STS-type cyclization to form mixed aliphatic-aromatic products (Figure 1c; Cook *et al.*, 2010). However, the plant ARSs characterized to date all formed products with relatively short side chains, derived from short-, medium- or long-chain acyls. Corresponding enzymes forming cuticular wax alkylresorcinols, with C_{17}–C_{25} alkyl side chains, have not been described to date.

© 2020 The Authors.

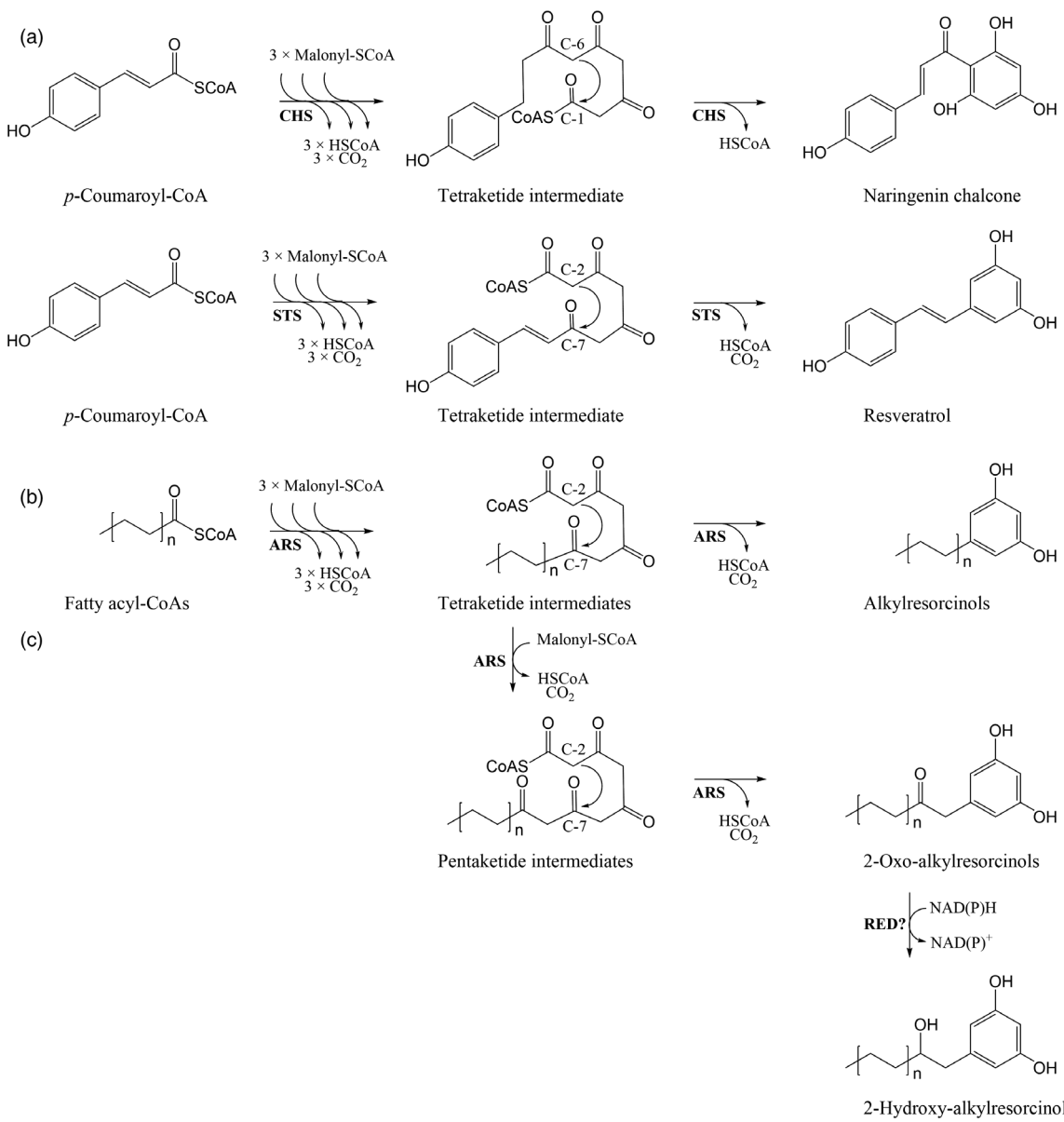

Figure 1. Reaction sequences catalyzed by plant type-III polyketide synthases.
(a) Chalcone synthases (CHSs) use coumaroyl-CoA starter substrate for three consecutive condensations with malonyl-CoA, to form a tetraketide intermediate that is then cyclized through a C-6 → C-1 Claisen condensation into chalcone (the mechanistic arrow in the tetraketide structure indicates nucleophilic attack of C-6 to C-1, leading to C-C bond formation). Stilbene synthases (STSs) use coumaroyl-CoA for three condensations with malonyl-CoA to form the same tetraketide intermediate as CHS, but then cyclize it through a C-2 → C-7 aldol condensation (C-C bond formation between C-2 and C-7) into stilbenes (e.g. resveratrol).
(b) Alkylresorcinol synthases (ARSs) use fatty acyl-CoAs of various chain lengths as starter substrates for condensation with three malonyl-CoAs and aldol cyclization analogous to STS.
(c) ARSs can catalyze an additional malonyl-CoA condensation to form pentaketide intermediates that will then be cyclized into 2-oxo-alkylresorcinols. The latter may be transformed into 2-hydroxy-alkylresorcinols by unknown reductases.

Based on the previous knowledge on plant PKSs, the present study aimed to identify an ARS enzyme responsible for formation of the alkylresorcinols accumulating in cuticular wax mixtures of rye. In particular, our goals were: (i) to isolate a candidate PKS gene encoding an enzyme that likely catalyzes STS-type cyclization; (ii) to characterize the product spectrum of the enzyme in terms of ring structures formed; (iii) to test in how far it accepts acyl-CoA starters with varying chain lengths; (iv) to investigate the subcellular localization of the enzyme and its expression patterns across plant organs; and (v) to correlate its expression levels with the amounts of cuticular alkylresorcinol products.

© 2020 The Authors.
The Plant Journal © 2020 John Wiley & Sons Ltd,

RESULTS

The goal of the present investigation was to isolate and characterize the PKS enzyme(s) involved in forming very-long-chain alkylresorcinols found in the cuticular waxes of *S. cereale*. To this end: we (i) cloned a candidate type-III PKS by homology-based polymerase chain reaction (PCR) and assessed its subcellular localization; (ii) characterized the encoded enzyme using yeast expression and gas chromatography-mass spectrometry (GC-MS) analysis of the resulting lipids; (iii) correlated gene expression with product accumulation patterns during leaf development; and (iv) further compared gene expression levels in various organs with corresponding alkylresorcinol amounts.

PCR-based isolation of a candidate rye PKS gene and subcellular localization

To isolate putative ARS genes from *S. cereale*, mRNA was isolated from leaves of 3-week-old plants and reverse-transcribed into cDNA. Gene-specific forward and reverse primers (Table S1) were designed based on sequence regions that had been found conserved among all previously isolated grass ARSs, while differing from CHSs of the same species (Figure S1a). PCR amplification of the cDNA template with these primers yielded a product with the expected size of approximately 1000 bp, and 5′ and 3′ Rapid Amplification of cDNA Ends (RACE) reactions were used to extend it. Sub-cloning and sequencing demonstrated that the resulting cDNA, tentatively designated as *ScARS*, comprised an open reading frame (ORF) of 1230 bp that encoded a 43.3 kD protein of 409 amino acids. The entire target sequence was also amplified from *S. cereale* genomic DNA (gDNA), and comparison between cDNA and gDNA sequences showed that the *ScARS* gene consisted of two exons of 218 and 1012 bp, separated by an intron of 91 bp (Figure S1b,c). The obtained gDNA sequence was used to BLAST-search the *S. cereale* genome database (Bauer *et al.*, 2017), retrieving one genomic DNA record, Sc4Loc00303157, with only a few nucleotide mismatches leading to two amino acid changes in the translated protein sequences (residues 306 and 310). Two GenBank records of complete CDSs, MF033355.1 and MH513639.1, from different cultivars of *S. cereale* had high sequence similarity to *ScARS* (Figure S1d) but lacked a biochemical characterization. All taken together, we considered these three database sequences as allelic to *ScARS*, with single nucleotide polymorphisms (SNPs) likely due to different cultivar backgrounds.

The predicted ScARS protein sequence comprised residues thought to be involved in substrate binding and catalysis in all plant type-III PKSs characterized to date (Figure 2). Most importantly, the ScARS sequence contained a stretch of amino acids implicated in directing aldol cyclization analogous to STSs, rather than the Claisen condensation occurring in CHSs (Austin *et al.*, 2004; Cook *et al.*, 2010). Accordingly, phylogenetic analyses showed that the ScARS amino acid sequence clustered with the other monocot ARS sequences known to date, separate from the CHSs of rye, other monocots and diverse dicots (Figure 3). Overall, ScARS had 58–62% amino acid sequence identity with the ARSs from *S. bicolor* and *O. sativa*, and only 46–47% identity with the two previously characterized *S. cereale* CHSs (Table S2). These results, taken together, suggested that ScARS has a biochemical function different from CHS type-III PKS enzymes.

The Dense Alignment Surface (DAS) algorithm (http://www.sbc.su.se/~miklos/DAS; Cserzö *et al.*, 1997) predicted up to four lipophilic segments in ScARS but no trans-membrane domains (Figure S1c). To assess whether ScARS is associated with the membranes of the ER and thus has access to acyl-CoA substrate pools, we investigated the subcellular localization of the enzyme. To this end, the ScARS protein was N- and C-terminally fused to green fluorescent protein (GFP), and the resulting protein constructs were transiently expressed in *Nicotiana benthamiana* under control of the 35S promoter. The transgenic tobacco epidermis cells showed GFP fluorescence in a reticulate pattern coinciding with that of the ER-specific marker HDEL (Figure 4), confirming that the ScARS protein was indeed localized to this cellular compartment.

Characterization of ScARS by heterologous expression in yeast

To test the biochemical activity of ScARS, the enzyme was expressed in yeast, and resulting lipids were analyzed by GC-MS. Yeast expressing *ScARS* contained several compounds not present in the empty-vector control, all of them

Figure 2. Amino acid sequence comparison between ScARS and select, previously characterized alkylresorcinol synthase (ARS) and chalcone synthase (CHS) enzymes.

Background shades of gray designate amino acids conserved at a given position in the multiple-sequence alignment. The catalytic-triad residues Cys164, His303 and Asn336 (numbering according to MsCHS2) characteristic of all plant type-III polyketide synthases (PKSs) are highlighted by asterisks, the residues involved in CoA binding are highlighted by triangles, and the residues implicated in functional diversity are highlighted by dots. The key residues associated with the C-2 → C-7 aldol condensation mechanism are marked by a line, and the amino acids related to hydrogen bonding during cyclization are labeled by numbers. MsCHS2: *Medicago sativa* chalcone synthase2; Gh2PS: AhSTS: *Arachis hypogaea* stilbene synthase; CsCHS: *Cannabis sativa* chalcone synthase; OsCHSs: *Oryza sativa* chalcone synthases; SbCHSs: *Sorghum bicolor* chalcone synthases; ScCHSs *Secale cereale* chalcone synthases; CsOLS: C. *sativa* olivetol synthase; SbARSs: *Sorghum bicolor* alkylresorcinol synthases; ScARS: *Secale cereale* alkylresorcinol synthase; OsARSs: *O. sativa* alkylresorcinol synthases; PpARS: *Physcomitrella patens* alkylresorcinol synthase (see Table S8 for accession numbers of genes).

© 2020 The Authors.

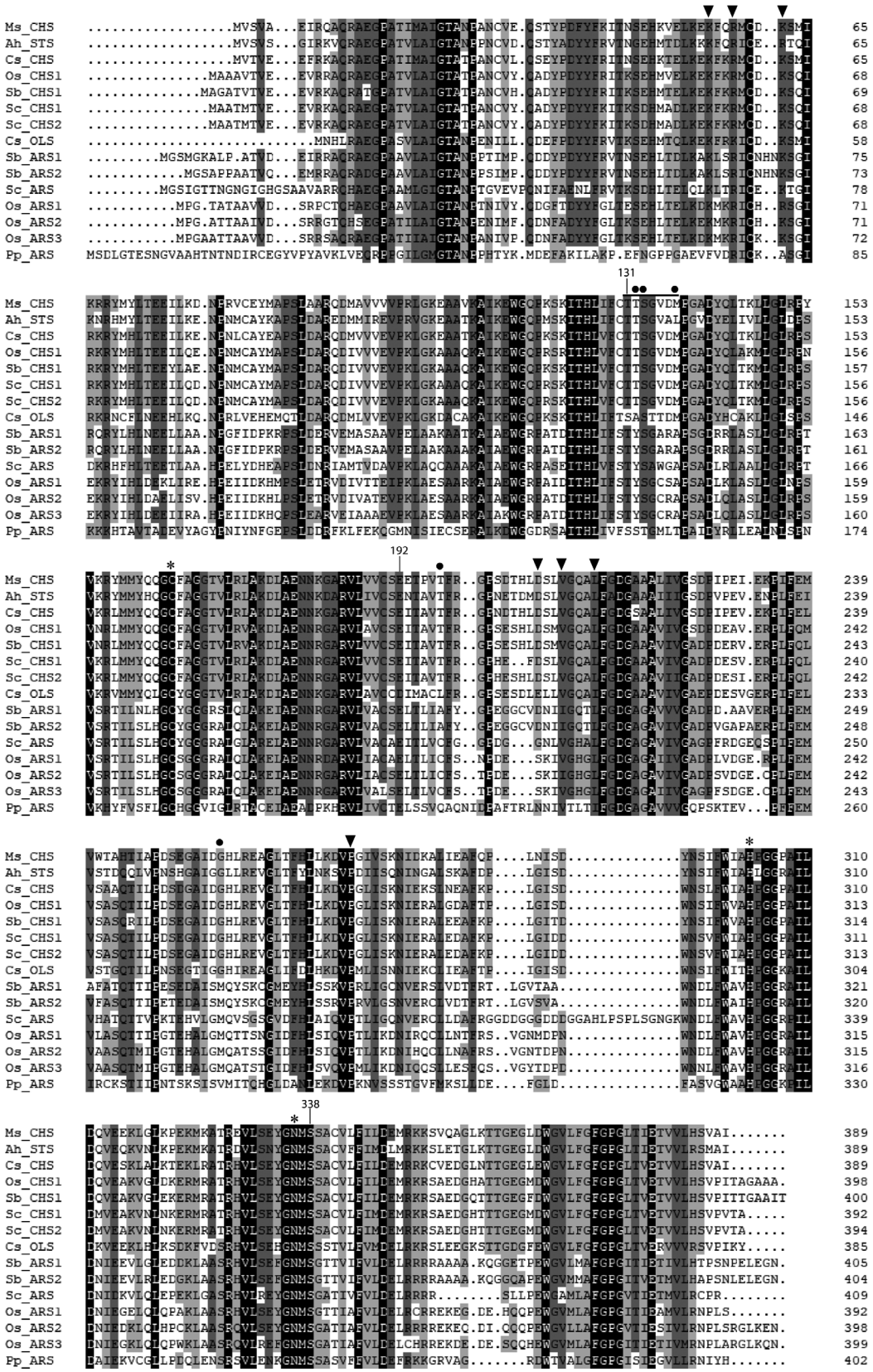

© 2020 The Authors.
The Plant Journal © 2020 John Wiley & Sons Ltd, *The Plant Journal*, (2020), doi: 10.1111/tpj.14704

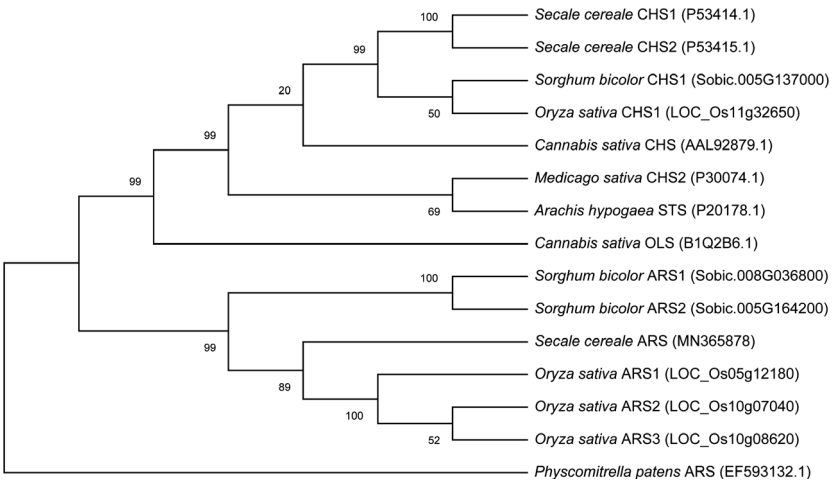

Figure 3. Phylogenetic relationship between *Secale cereale* alkylresorcinol synthase, ScARS, and select other plant type-III polyketide synthases (PKSs). Amino acid sequences were compared between ScARS, other ARSs from monocots and the moss *Physcomitrella patens*, and further type-III PKSs [chalcone synthases (CHSs)/stilbene synthases (STSs)] from gymnosperms, dicots and monocots.

found in the same fraction upon thin-layer chromatography (TLC) separation (silica, chloroform-ethyl acetate 7:3, v/v; Figure 5, top panel). One of them had MS fragmentation and GC retention characteristics identical to those of a synthetic standard of alkylresorcinol with unbranched, saturated C_{13} side chain (Figure 5, bottom panel) and was thus identified as 13:0 alkylresorcinol. Five more compounds in the same fraction, also with characteristic MS fragments *m/z* 73, 268 and 281, were accordingly identified as alkylresorcinol homologs with (unbranched) 9:0, 11:0, 14:0, 15:0 and 17:0 alkyl chains (molecular ions *m/z* 380, 408, 450, 464 and 492, respectively). Two more compounds in the yeast extract, also with characteristic alkylresorcinol MS fragments, had molecular ions $[C_6H_3(OTMSi)_2C_nH_{2n-1}]^+$ and corresponding fragments $[M\text{-}15]^+$ two mass units less than the saturated homologs. They were, thus, identified as unsaturated alkylresorcinols with 15:1 and 17:1 side chains. The double bond could not be localized within the alkyl chains based on the GC-MS characteristics of the TMSi ether derivatives analyzed here.

More detailed analyses of the total lipid extracts (without prior TLC fractionation) from yeast expressing *ScARS* revealed several more products with the characteristic MS fragment ion *m/z* 268, suggesting further alkylresorcinol structures (Figure S2a). Based on their apparent molecular ions *m/z* 506 and *m/z* 504, along with corresponding ions M-15 as well as carbonyl α- and β-fragments (Figure S2b,c), two of these compounds were tentatively identified as 5-(2′-oxo)-alkylresorcinols with 17:0 and 17:1 side chains, respectively. Two more compounds exhibiting the MS fragment *m/z* 268 in lesser relative abundance had molecular ions *m/z* 580 and *m/z* 578 together with corresponding ions M-15 and α-fragments, indicating the presence of a TMS-derivatized hydroxyl function (Figure S2d,e). All evidence taken together, these compounds were tentatively identified as 5-(2′-hydroxy)-alkylresorcinols with 17:0 and 17:1 side chains, respectively. Further hydroxyalkylresorcinol homologs with 15:0, 16:0, 18:0 and 19:0 alkyl chains were similarly identified as trace components (Figure S2a). Several of these alkylresorcinol-type structures had previously been found in rye, albeit using different extraction, separation and detection methods. In particular, MS fragmentation patterns had been reported in most cases for the alkylresorcinol compounds without prior derivatization of hydroxyl functions, except for one report mentioning a TMSi-ether derivative similar to those described here (Suzuki *et al.*, 1999). Possible further ScARS products, including chalcones, stilbenes and pyrones, could not be detected in the total lipid extract from yeast expressing *ScARS*, even with targeted searches for characteristic MS fragments.

The relative abundance of individual alkylresorcinols in the lipid extracts of wild-type yeast expressing *ScARS* was determined, without prior TLC fractionation, by integrating GC traces of the characteristic MS fragment *m/z* 268. The series of saturated alkylresorcinols was dominated by the 15:0 homolog, accompanied by moderate amounts of 11:0, 13:0 and 17:0 as well as minor quantities of 25:0 (Figure 6a). The unsaturated alkylresorcinols had a very similar chain length distribution, comprising mainly 15:1, minor amounts of 17:1, and traces of 16:1.

To assess the chain length distribution of the acyl substrates that may be available to ScARS upon expression in the wild-type yeast strain used here, we determined the acyl profile of its total neutral lipids as a proxy. To this end, the yeast acyl components of the neutral lipids were trans-esterified into fatty acid methyl esters (FAMEs), and the resulting products were analyzed by GC-MS. The pool of saturated acyls in the *ScARS*-expressing yeast comprised 14% 16:0 FAME and 4% 18:0, along with 0.5% 26:0 FAME and trace amounts of other homologs (Figure 6b). Thus, the overall lipid mixtures had an acyl chain length distribution very similar to the alkylresorcinols, but with one more carbon in the acyl than in the alkylresorcinol side chain as expected based on the predicted ARS reaction

© 2020 The Authors.

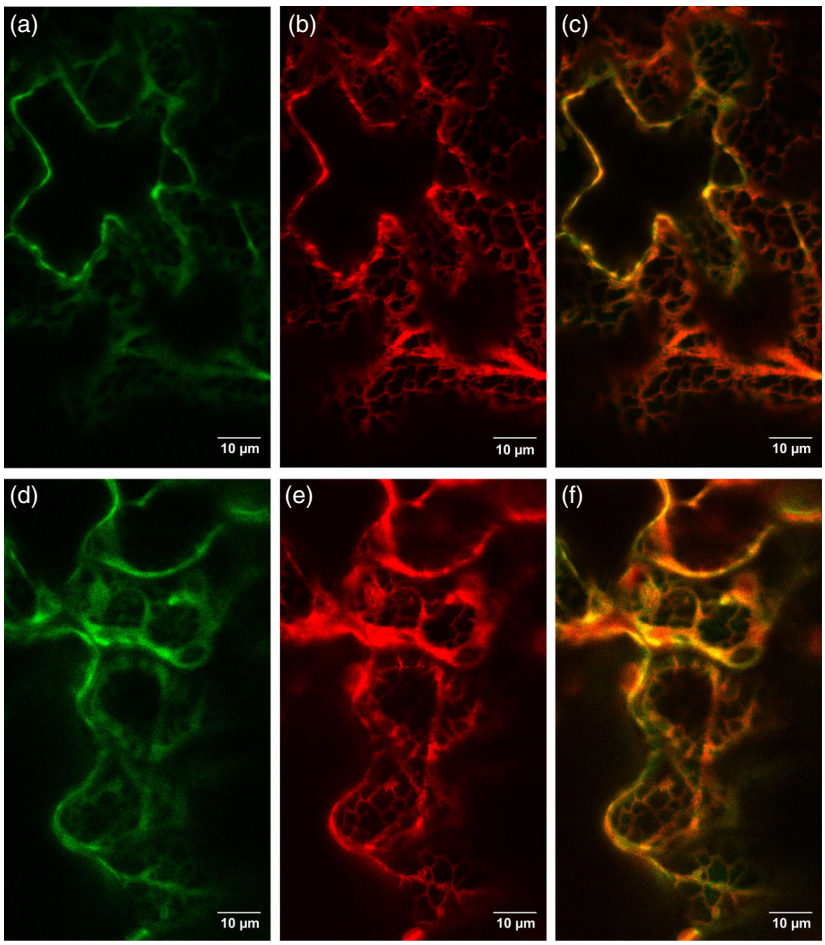

Figure 4. Subcellular localization of the ScARS protein.
(a) A N-terminal fusion of ScARS with GFP (35S:sGFP-ScARS) and (b) the endoplasmic reticulum (ER)-specific marker 35S:HDEL-RFP were transiently expressed in *Nicotiana benthamiana* epidermal cells; (c) merged image. (d) A C-terminal fusion of ScARS with GFP (35S:ScARS-sGFP) and (e) the ER-specific marker 35S:HDEL-RFP were transiently expressed in *N. benthamiana* epidermal cells; (f) merged image.

(Figure 1c). The FAME mixture further contained unsaturated acyls (about 65% 16:1, 23% 18:1, and traces of 17:1), in a distribution also similar to the chain lengths of corresponding unsaturated alkylresorcinols. However, the neutral lipids of the transgenic yeast comprised roughly equal quantities of saturated and unsaturated acyls overall, while the co-occurring ScARS product mixture contained much more saturated than unsaturated alkylresorcinols.

To test whether ScARS can catalyze the formation of alkylresorcinols with side chains longer than 19 carbons, we expressed it in a yeast strain with altered very-long-chain acyl composition. For this, we chose the *elo3*Δ yeast known to have levels of 20:0 and 22:0 acyls increased relative to wild type (Oh *et al.*, 1997), thus two substrates expected to yield 19:0 and 21:0 alkylresorcinols, respectively. Initially, FAME profiling of neutral lipids confirmed that, under our conditions, *elo3*Δ yeast had significantly increased levels of 20:0 and 22:0 acyls, concomitantly decreased levels of 16:0 and 18:0 acyls, and no detectable 26:0 acyl (Figure 6b). The *elo3*Δ yeast expressing *ScARS* contained alkylresorcinols with 9:0 to 21:0 side chains in a relative distribution resembling that of wild-type yeast expressing *ScARS* (Figure 6a). However, the mutant yeast transgenics had significantly increased 19:0 alkylresorcinol amounts compared with corresponding wild type, and substantial amounts of 21:0 alkylresorcinol accumulated only in the mutant background. Conversely, expression of *ScARS* in *elo3*Δ mutant yeast led to a decrease of 15:0 alkylresorcinol. Overall, the changes in ScARS product profiles between wild-type and mutant yeast thus paralleled the changes in FAME profiles between both backgrounds.

Correlation between alkylresorcinol accumulation and *ScARS* expression during leaf development

To assess whether ScARS may function *in planta* by forming the alkylresorcinols that accumulate in the rye leaf cuticle, we sought to compare the spatial and temporal expression patterns of *ScARS* with those of wax alkylresorcinol accumulation during organ development. Preliminary tests had shown that rye seedling wax mixtures contained substantial amounts of alkylresorcinols, suggesting that the seedling leaves could be used for our comparative investigations. We chose the second leaf (i.e. the first true leaf above the cotyledon) for analysis, as its expansion is highly reproducible, with rapid, linear growth to constant

© 2020 The Authors.
The Plant Journal © 2020 John Wiley & Sons Ltd,

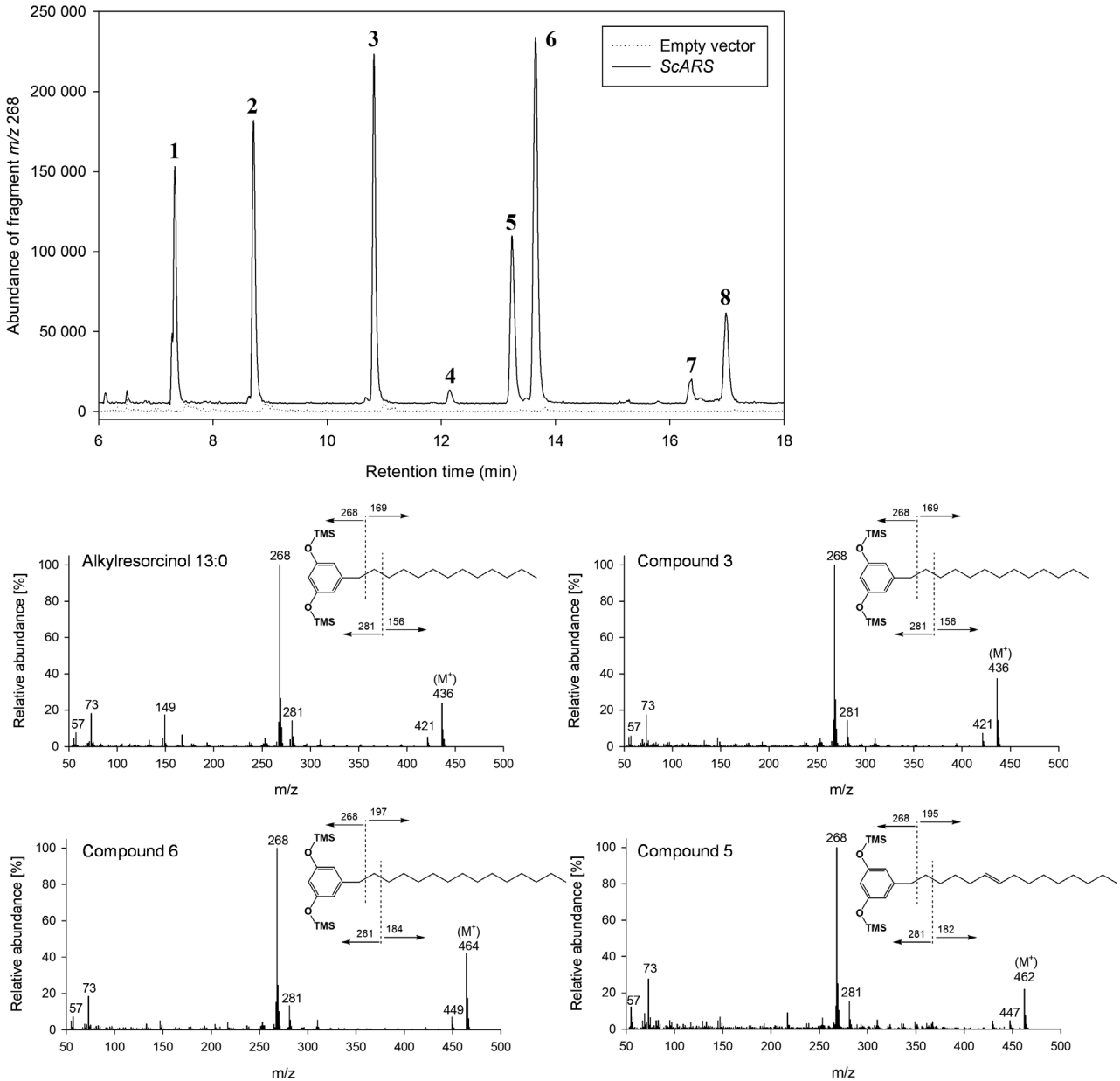

Figure 5. Analysis of alkylresorcinols from recombinant wild-type yeast expressing rye alkylresorcinol synthase, ScARS.
Yeast expressing either empty vector (pESC-URA) or *ScARS* (pESC-URA:*ScARS*) were extracted, and corresponding thin-layer chromatography (TLC) fractions were analyzed by gas chromatography-mass spectrometry (GC-MS) using select ion monitoring of fragment *m/z* 268. Compounds were identified as: **1**, 9:0 alkylresorcinol; **2**, 11:0 alkylresorcinol; **3**, 13:0 alkylresorcinol; **4**, 14:0 alkylresorcinol; **5**, 15:1 alkylresorcinol; **6**, 15:0 alkylresorcinol; **7**, 17:1 alkylresorcinol; and **8**, 17:0 alkylresorcinol. Mass spectra from peaks **3**, **6** and **5** are shown as representative examples for various alkylresorcinols formed by yeast expressing *ScARS*. The mass spectra of (TMSi-derivatized) authentic standard of 13:0 alkylresorcinol is compared with those of compounds **3**, **6** and **5.** Compound **3** showed a fragmentation pattern identical to that of the authentic 13:0 alkylresorcinol standard and was, thus, identified as 13:0 alkylresorcinol (molecular ion *m/z* 436). Compounds **6** and **5** were accordingly identified as 15:0 alkylresorcinol (molecular ion *m/z* 464) and 15:1 alkylresorcinol (molecular ion *m/z* 462). The double bond positions in the unsaturated compounds are tentatively assigned based on their likely fatty acyl-CoA precursors from yeast.

size. Furthermore, previous studies on barley had shown that wax accumulates most rapidly in the zone where the leaf blade emerges from the sheath of the lower, previous sheath (Richardson *et al.*, 2005), and the present analyses therefore focussed on the parts of the leaf blade beyond the point of emergence (POE). Three sets of experiments were carried out: (i) to monitor the growth of the second leaf by measuring the length and width of the exposed leaf blade as a function of time; (ii) to assess accumulation of surface compounds on the exposed leaf blade; and (iii) to quantify *ScARS* expression levels in corresponding tissue samples.

© 2020 The Authors.

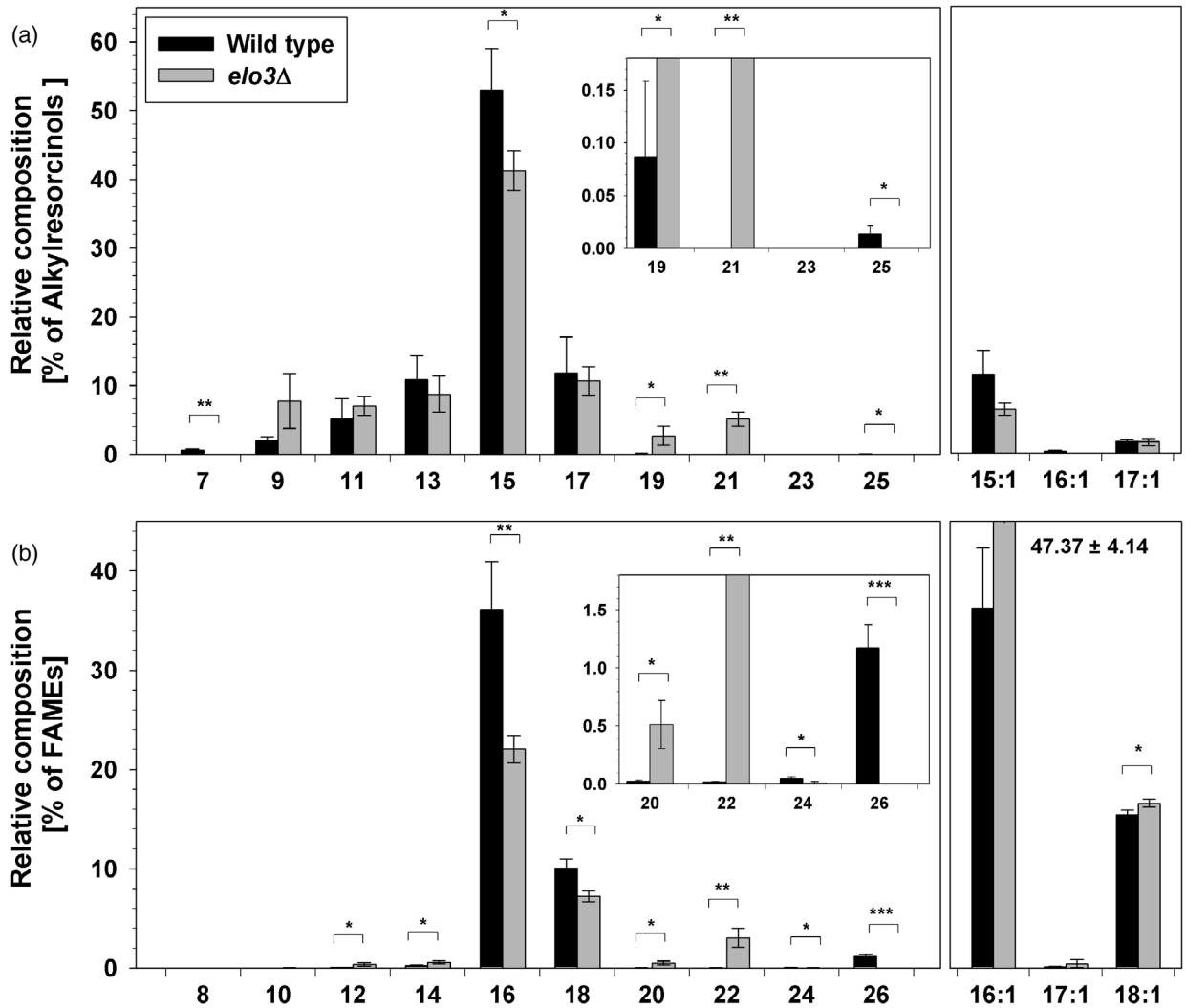

Figure 6. Quantitative analysis of the alkylresorcinols formed by yeast expressing rye alkylresorcinol synthase, ScARS.
(a) Relative amounts of alkylresorcinols with various saturated (left) and unsaturated (right) alkyl chains in wild-type and elo3 mutant yeast. The *x*-axis labels show carbon numbers of the alkyl chains. Alkylresorcinols were quantified by gas chromatography-mass spectrometry (GC-MS) using the selected ion *m/z* 268.
(b) Relative amounts of fatty acid methyl esters (FAMEs) with various saturated (left) and unsaturated (right) acyl chains in corresponding yeast lines. The *x*-axis labels show carbon numbers of the acyl chains. FAMEs were quantified by GC-MS using the selected ion *m/z* 74. All values are given as means ($n = 3$) ± SD, asterisks indicate significant differences between the two yeast lines detected by Student's *t*-test (*$P < 0.05$; **$P < 0.01$).

To monitor the expansion of the second leaf, its blade length was measured as the distance between leaf tip and the POE from the sheath of the previous leaf (Figure S3a). The blade length increased steadily over the course of almost two weeks, with linear growth of about 1.8 cm day^{-1}, and then plateaued at about 21 cm (Figure S3b). In contrast, the blade width at the POE remained constant over the whole time interval. For detailed wax and gene expression analyses, four different time points spanning the linear phase of leaf growth were selected and designated as stages I–IV. Accordingly, leaves were harvested on days 7, 10, 13 and 16, with exact lengths of 7, 10, 15 and 20 cm, respectively. Leaf blades harvested at growth stages I–III were cut into 1-cm segments, and those sampled at stage IV into 2-cm segments (Figure S3c).

The cuticular waxes from each segment of the rye leaf two (i.e. the first true leaf) were analyzed independently for all four growth stages. Across young (stage I) leaf blades, the total amounts of wax increased from 6 μg cm^{-2} near the POE (on the segment 5–6 cm from the leaf tip) to 9 μg cm^{-2} near the middle of the blade (segment 3–4 cm from the leaf tip), whereas the further blade sections towards the tip all showed constant wax loads (Figure 7a). Thus, the spatial distribution of wax along the leaf axis indicated that wax biosynthesis in young leaves occurred mainly within the lower leaf sheath and continued only slightly past the POE. Similarly, older blades (stages II–IV)

© 2020 The Authors.

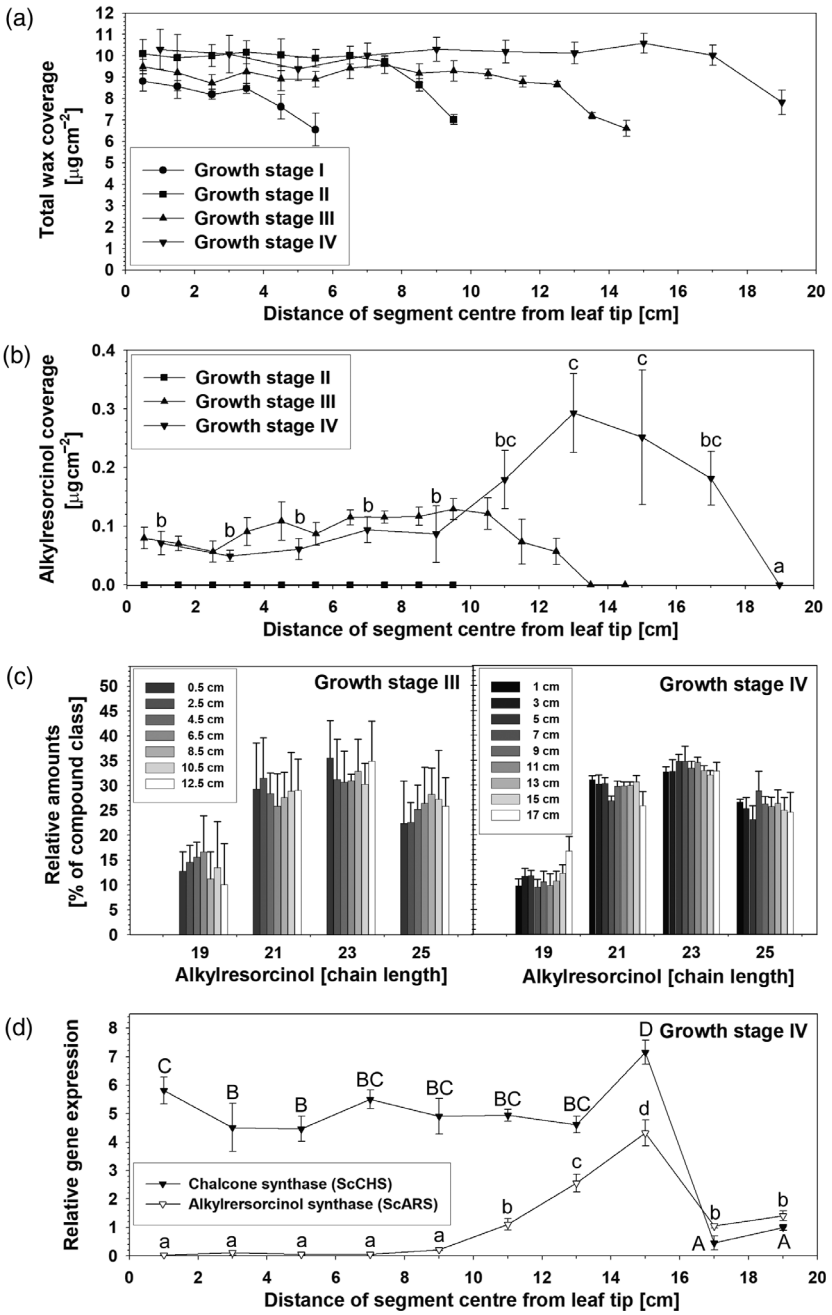

Figure 7. Spatial distribution of cuticular alkylresorcinols and alkylresorcinol synthase (ARS) expression across the second rye leaf.
(a) Total wax coverage on each leaf segment in growth stages I–IV.
(b) Total alkylresorcinol coverage within the wax mixtures on each leaf segment in growth stages II–IV. Amounts given in (a) and (b) are averages with standard deviations of six independent parallels.
(c) Chain length distribution within the alkylresorcinol fraction within cuticular waxes on each leaf segment in growth stages III and IV. The *x*-axis labels indicate alkyl chain lengths.
(d) Quantitative reverse transcriptase-polymerase chain reaction (qRT-PCR) analysis of *ScARS* and *ScCHS* gene expression levels as a function of position along the leaf blade in growth stage IV. Gene expression was normalized against *18S rRNA* and the expression value of ScARS in the 18–20-cm segment. The relative expression levels are given as mean values ($n = 3$) ± SD. The *x*-axis labels in (a), (c) and (d) represent the distance of the leaf segment centers from the leaf tip. Alkylresorcinol coverages in growth stage IV shown in (b) and expression levels of *ScCHS* (uppercase letters) and *ScARS* (lowercase letters) shown in (d) were statistically analyzed by one-way ANOVA and Tukey's *post hoc* test ($P < 0.05$).

had wax coverages of 6–8 μg cm^{-2} near the POE that increased to 9–10 μg cm^{-2} about 3 cm past the POE, and then remained constant across the rest of the blade towards the tip. Taken together, these results showed that a zone of active wax biosynthesis around the POE was maintained throughout leaf development. Due to the intercalar growth at the base of the monocot leaf, which pushes epidermal cells away from the base and past the POE, this stationary wax accumulation zone must consist of a succession of epidermal cells over time. Our finding of similar wax coverages across all developmental stages, both at the POE and the blade tip, showed that all epidermal cells successively moved through the wax-forming zone and, there, accumulated similar wax amounts with similar rates. Because the leaf was expanding at a rate of 1.8 cm day^{-1}, it can be inferred that epidermal cells were accumulating 2–3 μg cm^{-2} wax in about 1.5 days after emergence, with a rate of approximately 1.5 μg cm^{-2} per day.

Within the wax mixtures of all blade segments and growth stages, seven compound classes were identified, leaving only about 10% of the mixtures unidentified

© 2020 The Authors.

(Figure S4). Waxes at all time points and blade positions had very similar compound class distributions, consisting predominantly of primary alcohols along with fatty acids, alkyl esters, aldehydes and alkanes, as well as traces of secondary alcohols and terpenoids. Thirty-four compounds were identified within the aliphatic classes, all with fully saturated, unbranched hydrocarbon chains. The series of C_{24}–C_{26} fatty acids and C_{24}–C_{28} primary alcohols were dominated by even-numbered homologs peaking at C_{26}, and C_{40}–C_{46} alkyl esters by isomers containing C_{26} alcohol linked to C_{16} and C_{18} fatty acids. In contrast, mainly odd-numbered alkanes in the range C_{27}–C_{33} were found, with slight predominance of C_{27}. Only C_{33} secondary alcohols with hydroxyls on C-14 and C-16 were present, and β-sitosterol was the only alicyclic compound detected. The relative amounts of homologs and isomers within compound classes did not vary significantly between leaf growth stages and segment positions on the leaf blade.

In the wax mixtures on blades at growth stages I and II (Figure 7b), no alkylresorcinols could be detected. In contrast, blade wax at stage III contained alkylresorcinols, with moderate coverages of about 0.1 μg cm^{-2} on all segments up to 11 cm away from the leaf tip (Figure 7b). Further segments closer to the POE (11–13 cm from the tip) had steadily decreasing alkylresorcinol amounts, while in the zone next to the POE no alkylresorcinols could be detected. The wax mixtures at stage IV had constant low alkylresorcinol coverages (about 0.1 μg cm^{-2}) across the entire distal portion of the leaf blade (0–10 cm from the tip), and significantly higher amounts (0.2–0.3 μg cm^{-2}) in segments 10–18 cm from the tip (i.e. 2–10 cm from the POE), but no alkylresorcinols in the segment near the POE (18–20 cm from the tip).

Within the alkylresorcinol fraction, seven homologs with unbranched, saturated side chains ranging from C_{19} to C_{25} were identified, in a fairly broad distribution peaking around C_{23} (Figure 7c). Alkylresorcinols with even-numbered side chains were detected only at trace levels. This homolog profile did not vary over time or as a function of the position along the leaf axis. Other resorcinolic structures, like 2OARs or 2HARs, could not be detected in the wax extracts.

Finally, the accumulation patterns of alkylresorcinols within the wax mixtures of various segments of the rye leaf blade were compared with the expression patterns of *ScARS*. To this end, *ScARS* expression was monitored using quantitative reverse transcriptase (qRT)-PCR across segments of the blade at growth stage IV, when alkylresorcinol formation was maximal according to our previous chemical analyses. *ScARS* was not expressed in the distal half of the blade (0–8 cm from the tip), at relatively high levels in segments 12–16 cm from the tip (i.e. 4–8 cm from the POE), and at low levels near the POE (16–20 cm from the tip; Figure 7d). To put the *ScARS* expression pattern into context, another type-III PKS, ScCHS, forming chalcone as the central intermediate along the ubiquitous flavonoid and lignin pathways was assessed. *ScCHS* was expressed highly across all blade segments 0–16 cm from the tip (i.e. > 4 cm from the POE) and at low levels near the POE, thus showing an expression pattern distinct from *ScARS*.

Comparison between ScARS expression and alkylresorcinol accumulation patterns across rye organs

To further confirm the involvement of *ScARS* in wax alkylresorcinol formation, the expression pattern of this gene was also compared with product accumulation profiles across various rye organs, including awn, glume, seed coat, peduncle, flag leaf blade, flag leaf sheath, stem, seedling leaf blade and root. While the wax coverages on most organs could be quantified on a surface area basis, thus enabling comparisons with literature data, the waxes on a few organs had to be assessed per dry weight (DW) due to their complex surface geometries. Overall, the flag leaf sheath, peduncle, glume and awn showed relatively high wax coverages, in contrast to the seedling leaf and root (Tables S3 and S4).

In the cuticular wax mixtures of all organs, the typical wax compound classes such as fatty acids, primary alcohols, alkyl esters, aldehydes and alkanes were detected (Tables S3 and S4). The waxes on the flag leaf blade and seedling leaf blade were dominated by primary alcohols, whereas glume and root surfaces accumulated predominantly alkanes and triterpenoids, respectively. Additionally, β-diketones and 2-alkanol esters were also found on most rye organs, the former dominating the mixtures on peduncle, flag leaf sheath, stem, awn and glume. Most compound classes showed similar chain length distribution across different organs, except for roots with distinctly limited compound classes and chain length range (Tables S5 and S6).

Alkylresorcinols were present in the wax mixtures of all organs analyzed, except for the root. They accumulated to relatively high levels on the flag leaf blade, flag leaf sheath and peduncle, to moderate amounts on the stem, awn and glume, and to low amounts on the seedling leaf blade and seed coat (Figure 8a,b). The alkylresorcinol homolog profiles differed slightly between organs, with C_{23} being the dominant side chain length on the peduncle, flag leaf blade, flag leaf sheath, stem, awn and glume, C_{21} in the seed coat, and both C_{21} and C_{23} in similar amounts on the seedling leaf blade (Tables S7 and S8).

Finally, to further test the *in planta* biochemical function of *ScARS*, the expression levels of *ScARS* in various rye organs were assessed by qRT-PCR. The gene was found most highly expressed in flag leaf blade tissue, moderately in the flag leaf sheath, significantly less in the peduncle and stem, and even lesser in the seed coat, seedling leaf

© 2020 The Authors.

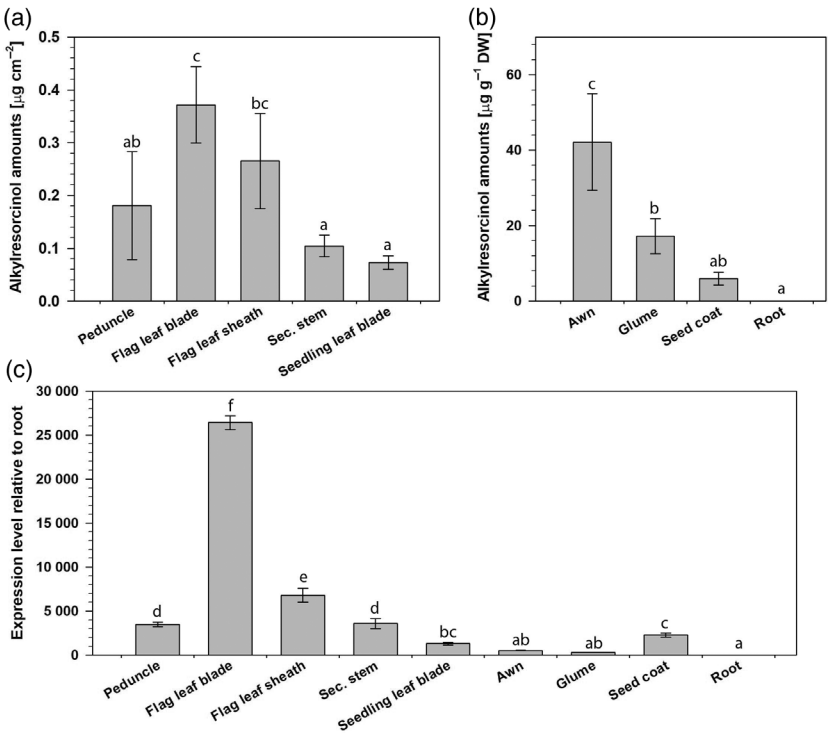

Figure 8. Spatial distribution of cuticular alkylresorcinols and alkylresorcinol synthase (ARS) expression across various organs of rye.
(a) *ScARS* expression in different rye organs quantified by quantitative reverse transcriptase-polymerase chain reaction (qRT-PCR). Gene expression was normalized against *18S rRNA* and the expression value of *ScARS* in the root.
(b) Alkylresorcinol amounts quantified against surface area for peduncle, flag leaf blade, flag leaf sheath, stem and seedling leaf blade.
(c) Alkylresorcinol amounts quantified against dry weight (DW) for awn, glume, seed coat and root. All alkylresorcinol amounts and *ScARS* expression levels are given as mean values ($n = 4$) ± SD. Data were statistically analyzed by one-way ANOVA and Tukey's *post hoc* test ($P < 0.05$).

blade, awn, glume and root (Figure 8c). Overall, the organ-specific expression pattern of *ScARS*, thus, matched the accumulation levels of alkylresorcinols in different organs.

DISCUSSION

In the current study, we characterized a type-III PKS involved in the biosynthesis of cuticular alkylresorcinols in rye. We found that the enzyme, ScARS, has STS-type rather than CHS-type sequence characteristics, and that it forms STS-type resorcinol ring structures with high specificity. However, in contrast to other STS enzymes, ScARS accepts a broad range of acyl starter substrates, and its association with the ER may enable access to very-long-chain acyl-CoA intermediates of wax biosynthesis. Accordingly, the temporal and spatial expression patterns of *ScARS* were correlated with cuticular alkylresorcinol accumulation in rye organs and during leaf development. Based on these overall findings, we can now discuss the biochemical characteristics of ScARS and its *in planta* function in more detail.

Biochemical characteristics of *ScARS*

The primary protein sequence of ScARS has several hallmarks common to plant type-III PKSs in general, and to STS-like PKS enzymes in particular (Figure S5). To assess the features of ScARS in detail, its sequence may be compared against that of CHS from *Medicago sativa,* MsCHS2, a PKS whose key amino acids for substrate binding and catalysis have been established based on crystal structure information. Accordingly, ScARS possesses the catalytic triad, Cys164, His303 and Asn336 (numbering in MsCHS2), conserved in all PKS superfamily members for substrate binding and catalysis of the decarboxylative condensation reactions. Similarly, ScARS also shares the amino acids thought to be involved in binding the CoA moieties of substrates and conserved between all previously characterized CHSs, STSs and ARSs. Therefore, ScARS may be expected to be an active PKS enzyme.

The ScARS sequence was also found to contain a stretch of amino acid residues thought to be crucial for hydrogen bonding in cyclization by STS-type C-2 → C-7 aldol condensation, distinct from CHS-type enzymes catalyzing C-6 → C-1 Claisen condensation (Austin *et al.*, 2004; Cook *et al.*, 2010). Thus, the ScARS sequence details suggest that it functions as an ARS enzyme. However, while the ScARS sequence shares various features with STS-type enzymes, it also differs from them in several residues crucial for enzyme function and substrate/product specificities, especially such amino acids known to surround the enzyme active site in the tertiary structure of MsCHS2 (Austin *et al.*, 2004). For example, the MsCHS2 residues Thr-132, Met-137, Thr-197 and Gly-256 are replaced by Tyr, Ala, Cys and Met in ScARS, respectively. The other ARS enzymes characterized before have amino acids similar to those of ScARS in these positions, possibly to enable binding of aliphatic fatty acyl-CoAs instead of bulky aromatic starters. All taken together, the primary sequence of ScARS

© 2020 The Authors.

thus suggested an active PKS enzyme specifically forming resorcinolic products.

The predicted resorcinol-forming activity of ScARS was (in the absence of rye mutants or overexpressor plants) tested using yeast heterologous expression. In the lipid extracts from yeast expressing ScARS only resorcinolic structures and no chalcones could be detected, thus confirming that the enzyme has STS-type (C-2 → C-7 cyclization) rather than CHS-type (C-6 → C-1 cyclization) activity. It should be noted that corresponding pyrones could not be detected, even though they have frequently been reported as (mechanistic derailment) side products of PKS enzymes. All resorcinolic structures detected in the transgenic yeast contained alkyl side chains, further showing that the enzyme prefers aliphatic over aromatic acyl starter substrates, and that it, therefore, has ARS and not STS activity. Overall, the lack of side products reveals high specificity of the ScARS enzyme both for the substrate used (i.e. aliphatic starters) and the products formed (i.e. resorcinolic ring structure).

Despite the overall high cyclization product specificity, the ScARS protein was found to produce trace amounts of pentaketide side products, 2OARs and 2HARs, implying that the enzyme may occasionally catalyze four instead of three condensations with malonyl extender units. Interestingly, similar variation in elongation round numbers had been reported for other ARSs before, where *P. patens* PpORS produced tetraketide as well as pentaketide products (Kim *et al.*, 2013), while sorghum SbARSs and rice OsARSs generated mainly tetraketides (Cook *et al.*, 2010). It is noteworthy that the pentaketides found here as side products of ScARS had previously been reported from rye grain extracts (after TLC separation; Seitz, 1992; Suzuki *et al.*, 1999). The ratio between alkylresorcinol (i.e. tetraketide) and 2OAR/2HAR (i.e. pentaketide) amounts in our yeast analyses was very close to that reported for rye grains, suggesting that both product types are formed by the same enzyme, ScARS.

Our yeast expression analyses shed further light on the substrate and product specificities of ScARS. On the one hand, ScARS was found to accept both saturated and unsaturated acyl substrates. To assess possible preferences of the enzyme between these different substrates, we profiled the acyl distribution within the total lipid pools of our transgenic yeast strains (as FAMEs). Our results show that the ratios of saturated and unsaturated compounds differ markedly between the total acyl pool and the alkylresorcinol products, suggesting that ScARS discriminates strongly against unsaturated acyl-CoA substrates for formation of the major alkylresorcinols (i.e. tetraketide products). Interestingly, more unsaturated substrates were incorporated into 2OARs and 2HARs (i.e. pentaketide products), possibly because subtle differences in binding of unsaturated acyl substrate may lead to differences in substrate conformation within the enzyme active site, leaving slightly more space to accommodate one more malonyl extender unit and/or delaying the ring-forming aldol condensation. The overall preference of ScARS for saturated acyl substrates distinguishes it from the sorghum ARSs previously described, which have high activity on mono- or even multi-unsaturated fatty acyl-CoAs (Cook *et al.*, 2010).

On the other hand, ScARS was also found to form alkylresorcinols with side chain lengths varying widely from C_7 to C_{25}, for this likely using C_8 to C_{26} acyl-CoA substrates. The wild-type yeast background was found to have acyl chain length ranges and distributions very similar to the corresponding alkylresorcinol distribution, suggesting that ScARS product profiles directly reflect the composition of available substrate pools and that, conversely, the enzyme has relatively little substrate chain length specificity. This was confirmed by analyses of *elo3*Δ mutant yeast expressing ScARS, where shifts in the chain length distributions of acyl pools led to similar shifts in chain length profiles of alkylresorcinol products. Taken together, our results show that ScARS accepts a broad range of mid-chain ($C_{8–14}$), long-chain ($C_{16/18}$) and very-long-chain ($C_{>20}$) fatty acyl-CoAs. Among these, the latter are most important, demonstrating that the enzyme is able to form very-long-chain alkylresorcinol products, including those accumulating in the cuticular waxes on various rye organs.

ScARS diverts wax biosynthesis intermediates into a short, distinct branch pathway forming cuticular alkylresorcinols

To test whether ScARS is indeed involved in forming the alkylresorcinols accumulating in rye surface waxes, and thus to verify its *in planta* function, we sought to establish temporal and spatial correlations between *ScARS* expression patterns and cuticular alkylresorcinol amounts. In a first experiment, a characteristic distribution of alkylresorcinols across the developing leaf blade was found, with highest product accumulation in segments about 5 cm away from the POE from the previous leaf's sheath. Expression of the *ScARS* gene peaked in the same leaf segments where alkylresorcinols accumulated to the highest concentrations, in a pattern distinct from a ubiquitous control gene, *ScCHS*. In contrast, the accompanying wax compounds ($C_{>26}$ fatty acids and their derivatives) showed a distribution markedly different from the alkylresorcinols, with highest product accumulation at or very near the POE, and expression of wax biosynthesis genes in grass leaves is known to peak in the same region around the POE (Richardson *et al.*, 2005). Taken together, our results thus show that formation of cuticular alkylresorcinols occurs in a leaf blade region distinct from that of other wax compounds, further removed from the POE and thus slightly later in epidermal cell development. The matching

© 2020 The Authors.
The Plant Journal © 2020 John Wiley & Sons Ltd,

patterns of alkylresorcinol accumulation and *ScARS* expression, both lagging wax accumulation and wax synthesis gene expression, respectively, suggest that *ScARS* is directly involved in formation of the cuticular alkylresorcinols.

To further confirm the role of *ScARS* in formation of cuticular alkylresorcinols, we compared gene expression and product accumulation across organs. A good correspondence between *ScARS* transcript levels and alkylresorcinol coverages (expressed in units of $\mu g\ cm^{-2}$) was found for the peduncle, flag leaf blade, flag leaf sheath, stem and seedling leaf blade. Among the other organs, for which alkylresorcinol concentrations were quantified on tissue DW basis (in units of $\mu g\ g^{-1}$), only a weak correspondence between product accumulation and gene expression levels was found. However, it should be noted that respective organs have complex structures comprising various surface tissues and types of cells, only some of which may express *ScARS*, substantially biasing the comparison between product amounts determined relative to whole-organ DWs.

Furthermore, the alkylresorcinol coverage of about 0.43 $\mu g\ cm^{-2}$ on the flag leaf blade, based on the specific leaf area of 32 $m^2\ kg^{-1}$ reported for rye (Tribouillois *et al.*, 2015), corresponds to a concentration of about 140 $\mu g\ g^{-1}$ DW, showing that the leaf accumulates higher alkylresorcinol concentrations than any other organ (including all those where concentrations were measured on a DW basis), further underpinning the good correlation between product amounts and ScARS expression levels. Therefore, we conclude that the *ScARS* is responsible for formation of the alkylresorcinols accumulating in the cuticular waxes covering various rye organs.

Our wax analyses matched previous literature showing that the alkylresorcinols on various rye organs had side chain lengths ranging only from C_{19} to C_{23} (Ji and Jetter, 2008). This narrow *in planta* product spectrum is in stark contrast to our yeast experiments, where ScARS accepted diverse substrate chain lengths to produce a broad series of homologous alkylresorcinols. Together, these findings suggest that a much narrower range of substrates may be available to the enzyme in rye compared with yeast. In particular, the different ScARS alkylresorcinol distributions in yeast and rye contexts may be due to differences in subcellular structures between the plant and the microorganism. In this context, it is important to note that ScARS was found localized to the ER *in planta*, based on our hydropathy analyses likely as a peripheral membrane protein (as it lacks long hydrophobic amino acid stretches to form transmembrane domains). It seems plausible that the ScARS protein may be associated in different ways with plant and yeast ERs, providing it access mostly to very-long-chain acyl-CoAs in the former and to medium/long-chain acyl-CoAs in the latter. Indeed, yeast acyl-CoA pools contain more C_8–C_{14} and unsaturated chains than those of plant cells (Færgeman *et al.*, 2001; Larson and Graham, 2001; Bach *et al.*, 2008), thus accounting for the higher amounts of medium/long-chain alkylresorcinols found in our yeast experiments compared with rye.

Interestingly, our yeast experiments also showed strong activity of ScARS on C_{16} and C_{18} acyl-CoAs, two substrates known to be very abundant in the plant ER (Stymne *et al.*, 1983; Stymne and Stobart, 1984; Abbadi *et al.*, 2004), yet no corresponding 15:0 alkylresorcinol and only small amounts of 17:0 alkylresorcinol were detected in rye cuticular waxes or total lipids (Deszcz and Kozubek, 2000; Magnucka *et al.*, 2007). These findings imply that the C_{16} and C_{18} acyl-CoAs are not available to the ScARS enzyme, possibly due to sequestration in different ER sub-compartments. Similarly, also acyl-CoAs with chain lengths of C_{28}–C_{32} (in some species up to C_{36}) are formed in the ER of plant epidermis cells (Suh *et al.*, 2005; Hegebarth *et al.*, 2017), and yet no corresponding 27:0–31:0 alkylresorcinols have been found in rye. On the one hand, these results may be explained by further ER sub-compartmentation, effectively separating pools of $C_{\leq 26}$ acyls and $C_{\geq 28}$ acyls. On the other hand, our results may also reflect differences in substrate affinities between various enzymes competing for the longer-chain acyl-CoA substrates. Most importantly, $C_{\geq 26}$ acyl-CoAs serve as substrates for further elongation and for modification into wax components such as alcohols, esters, aldehydes and free fatty acids. Our current rye wax analyses confirmed previous reports (Ji and Jetter, 2008) showing that respective wax compounds accumulate to quantities several orders of magnitude higher than the alkylresorcinols. These results indicate that the wax biosynthesis enzymes may well out-compete the ScARS enzyme for $C_{\geq 26}$ acyl-CoA substrates, in leaf blades even beyond the peak of wax biosynthesis near the POE. However, it can also not be ruled out that ScARS itself discriminates against starter substrates $C_{\geq 28}$ acyl-CoA. Further experiments are needed to test this, for example with yeast mutants producing fatty acyls longer than the C_{26} acyl-CoA found in the wild type.

Overall, our results describe ScARS as a highly product-specific enzyme, *in planta* utilizing fatty acyl-CoAs with a relatively narrow range of chain lengths in between the abundant $C_{16/18}$ acyls and the wax-specific $C_{26\text{-}32}$ acyls. This enzyme, thus, recruits specific fatty acyl elongation intermediates into a short branch pathway, to form mixed phenolic/alkyl products. Respective alkylresorcinols were detected in the surface waxes of almost all rye organs, with fairly similar chain length distributions. Based on the concomitant expression of *ScARS* in the same organs, it seems likely that this enzyme is involved in alkylresorcinol formation throughout the rye plant. The slight differences in the alkylresorcinol chain length profiles between organs may be due to differences in substrate availabilities, but

© 2020 The Authors.

they may also point to the presence of further ARSs with varying substrate chain length specificities. In this context, it is interesting to note that the rye genome encodes several proteins which, based on their primary sequences, are good candidates for further functional ARS enzymes. The draft genome loci Sc5Loc01798568, Sc5Loc01797658 and Sc5Loc00345447 are of particular interest.

Our results also imply that ScARS produces alkylresorcinols mainly destined for the cuticular wax coating various rye organs. Meanwhile, the accumulation patterns of alkylresorcinols in the wax, at least of leaf blades, differ markedly from those of all other wax constituents. Thus, the timing of alkylresorcinol biosynthesis (and *ScARS* gene expression) is largely independent of wax biosynthesis, pointing to autonomous regulation of both processes. Together, the tight regulation of alkylresorcinol biosynthesis and their dedicated formation for the plant surface raise important questions regarding their biological function(s) within the cuticular wax layer. However, only very little experimental evidence is available to answer these questions at the present time.

It has been surmised that the cuticular alkylresorcinols play a role in plant resistance in pathogen infection (García *et al.*, 1997). However, prior research found them accumulating exclusively in the intracuticular wax (Jetter and Schäffer, 2001; Ji and Jetter, 2008) and, thus, removed from the contact zone between plant tissue and pathogen cells. Therefore, it seems unlikely that the alkylresorcinols are involved in direct interaction with foreign organisms (e.g. pathogenic microorganisms, insect herbivores). Instead, the location of alkylresorcinols within the cuticle suggests that they may play a physiological role, likely in the context of the primary function of the plant cuticle to protect the tissue against non-stomatal water loss. Due to their mixed aliphatic/phenolic molecular structure, the very-long-chain alkylresorcinols are amphiphilic compounds and may be expected to act as surfactants in mixed lipophilic-hydrophilic systems. We, therefore, hypothesize that the cuticular alkylresorcinols may function as liners mediating contact between the carbohydrates/cutin subtending the cuticle and the much more lipophilic waxes deposited into/onto them.

Interestingly, alkylresorcinols occur in a wide range of plant species, especially in the Poaceae but also beyond (Barr *et al.*, 1988; Dring *et al.*, 1995; Zarnowski and Kozubek, 1999; Żarnowska *et al.*, 2000; Kienzle *et al.*, 2013). In many cases, they have been localized in surface tissues, frequently in the context of cuticular waxes (Richardson *et al.*, 2005; Ji and Jetter, 2008; Adamski *et al.*, 2013; Racovita *et al.*, 2016). Therefore, our current finding that an ARS enzyme is forming very-long-chain alkylresorcinols for accumulation in the surface waxes of rye may have implications for diverse other plant species with cuticular alkylresorcinols. We propose that many (if not all) of these species harbour at least one ARS-like enzyme dedicated to the formation of very-long-chain alkylresorcinols functioning in the cuticles covering their above-ground organs. These fairly widespread alkylresorcinols are thus distinct from those with shorter side chains found in single species, in many cases specifically formed by ARS-like enzymes in below-ground organs. For example, the alkylresorcinols accumulating in roots of etiolated rice seedlings showed high antifungal activity *in planta* (Suzuki *et al.*, 1996), while the alkylresorcinol derivative sorgoleone, produced by root hairs of sorghum, is thought to have allelopathic activity (Cook *et al.*, 2010). The corresponding ARS enzymes involved in formation of these diverse alkylresorcinol products thus reflect the evolutionary diversity and importance of this class of enzymes.

Conclusions

In this work, we characterized the PKS enzyme, ScARS, that forms the alkylresorcinols accumulating in the cuticular waxes on various organs of the rye plant. On the one hand, the enzyme has relatively little specificity for the aliphatic side chains of its products, due to the wide range of saturated and unsaturated acyl starters it accepts. The ScARS protein must have a special structure that can bind the very-long-chain starter substrates, likely in a relatively long, hydrophobic cavity. On the other hand, the ScARS enzyme is highly specific for the formation of the aromatic ring structure, and thus must have tight control over the conformation of the tetraketide intermediate prior to cyclization. We conclude that the active site pocket directing the malonate condensation steps as well as the ensuing cyclization reaction have a very specific volume and geometry. In this context, it will be interesting to test whether the same enzyme is also responsible for formation of other alkylresorcinol derivatives such as the co-occurring methylalkylresorcinols (with methyl branches on or near the aromatic head group). Such compounds are likely formed by incorporation of methylmalonate units instead of malonate, and thus slightly bigger substrates that need to fit into the same active-site cavity.

EXPERIMENTAL PROCEDURES

Plant growth conditions and sampling

Rye (*S. cereale* L. cv. Esprit) seeds were purchased from Capers, Vancouver, and germinated directly in soil. Plants were grown in several batches in plastic pots (diameter 15 cm) at a density of 18–22 per pot in a growth chamber (20°C, 24 h continuous light at 90–120 μmol m^{-2} sec^{-1}, relative humidity 70%). The second leaf emerged from the sheath of leaf one (the cotyledon) at day 5 after germination. Starting at that point, growth of leaf two was monitored daily by measuring the length of the blade beyond the POE.

For rye wax developmental analysis, the second leaves of three plants each were harvested at growth stages I (7 cm long, plant 7–8 days old), II (10 cm long, plant 9–11 days old), III (15 cm long,

© 2020 The Authors.
The Plant Journal © 2020 John Wiley & Sons Ltd,

plant 12–14 days old) and IV (20 cm long, plant 15–17 days old; Figure S3c). Only those with exact lengths of 7, 10, 15 and 20 cm were used for chemical analysis. Leaves harvested at stages I–III were cut into segments of 1 cm, while those from stage IV were cut into segments of 2 cm. Corresponding segments from three different leaves were pooled into one sample for wax extraction. Six independent parallels were analyzed for each position at each growth stage.

For rye organ wax analysis and gene expression comparison, rye cv. Xiaoheimai was grown at the experimental farm of Northwest A&F University, Yangling. Seedling leaf blade and root samples were harvested 30 days after germination; peduncle, flag leaf blade, flag leaf sheath, stem, awn, glume and seed coat were harvested 190 days after germination (15 days after pollination). Four independent parallels were analyzed for each organ.

Tobacco (*N. benthamiana*) plants used for *ScARS* transient expression were grown in growth chambers (22°C, 16 h light/8 h dark, at 90–120 μmol m^{-2} sec^{-1}, relative humidity 65%).

Wax extraction and chemical analysis

Wax extraction, sample preparation and analyses were performed using the method described by Ji and Jetter (2008). In brief, each plant sample was extracted twice for 30 sec with $CHCl_3$, supplemented with *n*-tetracosane as internal standard. The resulting solutions were concentrated, transferred into GC vials, and brought to dryness under nitrogen. The wax extracts were then subjected to derivatization by *N,O*-bis(trimethylsilyl)-trifluoroacetamide (BSTFA) in pyridine at 72°C for 45 min. The resulting products were dried under nitrogen and dissolved in $CHCl_3$ prior to analysis by GC-MS and GC-FID.

DNA, RNA extraction, RT-PCR and candidate gene isolation

DNeasy Plant Mini Kit (Qiagen, Toronto, Canada) was used for rye genomic DNA extraction. Total RNA was extracted from leaves of 4-week-old rye plants using a PureLink RNA mini kit (Invitrogen, Burlington, Canada) following the manufacturer's instructions. The resulting RNA was subjected to on-column DNA digestion by PureLink DNase Set (Invitrogen), and 1.5 μg of total RNA sample was reverse-transcribed to cDNA by Superscript II Reverse Transcriptase (Invitrogen) following the manufacturer's protocol. Phusion High-Fidelity DNA Polymerase (New England BioLabs, Whitby, Canada) was used in all amplification of DNA fragments used for cloning.

First, primers (ScARS-core-F and ScARS-core-R) specific to the ARS consensus sequences (Table S1) were used to amplify the core fragment of *ScARS*. Then, RACE was used to amplify the 5′- and 3′-ends flanking the core fragment. For 3′-end amplification, cDNA was synthesized with Adapter Primer (AP) using SuperScript II Reverse Transcriptase. The forward gene-specific primer ScARS-3RACE-F and the Abridged Universal Amplification Primer (AUAP) were used in the first PCR reaction. A nested-PCR was performed using the first-round PCR product as a template with the nested gene-specific forward primer ScARS-3nest-F and the AUAP. The resulting 3′-end PCR product was gel-purified, cloned into pCR-Blunt vector and sequenced. For 5′-end amplification, the 5′ RACE System for RACE kit (Invitrogen) was used. cDNA was synthesized using a gene-specific reverse primer ScARS-5RACE1-F. The gene-specific primer ScARS-5RACE2-F and Abridged Anchor Primer (AAP) were used in the first PCR reaction with the resulting cDNA. Another round of PCR was performed for the nested amplification with gene-specific primer ScARS-5nest-F and AUAP. The resulting PCR product was cloned and sequenced. The corresponding full-length cDNA and genomic DNA sequences of *ScARS* were amplified with gene-specific primers ScARS-BamHI-F and ScARS-XhoI-R from cDNA or genomic DNA, respectively. The resulting PCR products were cloned for Sanger sequencing.

Phylogenetic analysis

The amino acid sequence of ScARS was aligned with the amino acid sequences of previously annotated or characterized type-III PKSs (for accession numbers, see Table S9) from various bacterial, fungal or plant species using the MUSCLE algorithm (Edgar, 2004). The genomic sequences and corresponding annotations for *Triticum aestivum*, *Hordeum vulgare*, *Aegilops tauschii* and *Triticum urartu* were downloaded from the EnsemblPlants database, release version 44.0. The genomic sequences and the corresponding annotations for *S. cereale* were downloaded from the IPK database (https://webblast.ipk-gatersleben.de/ryeselect/downloads/), those of the remaining species were retrieved from the Phytozome database (Version 12.0). The following assemblies were used in the current research: *Arabidopsis thaliana* (Athaliana_167_TAIR10), *Brachypodium distachyon* (Bdistachyon_314_v3.1), *O. sativa* (Osativa_323_v7.0), *Setaria italica* (Sitalica_312_v2.2), *S. bicolor* (Sbicolor_313_v3.0) and *Zea mays* (Zmays_284_AGPv3). Phylogenetic trees were generated by MEGA10.0 with the neighbor-joining (N-J) method or EBI online software (https://www.ebi.ac.uk/Tools/msa/muscle/).

Quantitative PCR

For developmental analysis of gene expression, leaf segments were harvested at different growth stages. For gene expression comparison between different organs, peduncle, flag leaf blade, flag leaf sheath, stem, seedling leaf blade, awn, glume, seed coat and root were sampled. All RNA and cDNA samples were prepared as described above. The gene-specific primers ScARS-qRT-F, ScARS-qRT-R, ScCHS-qRT-F and ScCHS-qRT-R were used to measure gene expression levels, and 18S rRNA was quantified as a reference using primers Sc18S-qRT-F and Sc18S-qRT-R. qRT-PCR was performed in 10-μl reactions with BioRad iQ SYBR Green Supermix on a CFX Connect Real-Time System (Bio-Rad, Montreal, Canada) according to the manufacturer's instructions. Relative expression levels were calculated using $2^{-\Delta\Delta CT}$ method as described previously (Livak and Schmittgen, 2001). Four biological replicates were analyzed for each sample.

Tobacco transient expression and confocal microscopy

ScARS was cloned into pDONR221 entry vector (Invitrogen) by gene-specific primers, and the confirmed sequence was introduced into the GATEWAY binary vectors pGWB6 and pGWB5 using LR Clonase II enzyme mix (Invitrogen). The resulting constructs pGWB6-*p35S:GFP-ScARS-GFP* or pGWB5-*p35S:GFP-ScARS-GFP* were transformed into competent *Agrobacterium tumefaciens* GV3101 cells. Four-week-old *N. benthamiana* leaves were infiltrated with Agrobacteria carrying pGWB6-*p35S:GFP-ScARS* or pGWB5-*p35S:ScARS-GFP* according to the method described by Sparkes *et al.* (2006), and Agrobacteria harboring *p35S:HDEL-RFP* were co-infiltrated to serve as ER marker. Transformed plants were grown in a growth chamber for another 2 days, and an Olympus multiphoton confocal microscope was used to examine the fluorescence signals. GFP fluorescence was detected using excitation at 488 nm and emission collected at 509 nm; RFP fluorescence was detected using excitation at 543 nm and emission collected at 588 nm. The obtained data were analyzed by Olympus FLUOVIEW FV1000 software.

© 2020 The Authors.

Yeast assay and lipid analysis

The *ScARS* ORF was amplified from total cDNA by PCR with primers ScARS-BamHI-F and ScARS-XhoI-R, and cloned into pESC-URA vector. Yeast (*Saccharomyces cerevisiae*) wild-type strain INVSc1 (*MATa his3-D1 leu2 trp1-289 ura3-52*) or FAE-defective mutant strain *elo3*Δ (*MATa/α his3*Δ*1/his3*Δ*1 leu2*Δ*0/leu2*Δ*0 lys2*Δ*0/LYS2 MET15/met15*Δ*0 ura3*Δ*0/ura3*Δ*0 YLR372w::kanMX4/YLR372w::kanMX4*) were transformed with pESC-URA-*GAL1:ScARS* or pESC-URA using the LiAc/SS-DNA/PEG method (Gietz and Woods, 2002) and screened on minimal-medium agar plates lacking uracil. The recombinant yeast cells were cultivated in liquid minimal medium at 28°C overnight and transferred to liquid minimal medium supplemented with 2% (w/v) galactose to induce the expression of the target gene. After two more days of incubation, yeast cells were harvested for product analysis or FAME analysis.

For product analysis, yeast total lipids were extracted with chloroform-methanol (2:1, v/v; 20 volumes). The extract was washed with 0.9% NaCl (w/v; 0.2 volume), and the chloroform phase was transferred to a new tube and evaporated to dryness under a gentle stream of nitrogen gas. The lipid extracts were derivatized and analyzed by GC-MS as described above. Alkylresorcinols were quantified from extracted chromatograms of the fragment *m/z* 268. For FAME analysis, yeast pellets were washed in 2.5% NaCl (w/v; 0.2 volume) and then subjected to transmethylation by incubation at 85°C for 2 h with 0.1 volume of 0.5 M sulfuric acid in methanol containing 2% (v/v) dimethoxypropane. After cooling, 2.5% NaCl (w/v; 0.1 volume) was added, and the resulting FAMEs were extracted in 0.8 volume of hexane and analyzed by GC-MS with the following oven program: 50°C held for 2 min, raised by 40°C/min to 100°C and held for 2 min, raised by 3°C/min to 320°C and held for 5 min. FAMEs were quantified based on GC profiles using selected ion *m/z* 74 with correction factor of 4.08 to account for the lower ionization yield of unsaturated FAMEs.

ACKNOWLEDGEMENTS

The authors thank Drs Mathias Schuetz and Lacey Samuels (University of British Columbia) for providing the ER-specific marker *35S:HDEL-RFP*; Dr Pingchuan Deng (Zhejiang University) for technical support of phylogenetic analysis; and Alberto Ruiz Orduna (University of British Columbia) for assistance in mass spectrometric interpretation. This work has been supported by the Natural Sciences and Engineering Research Council (Canada), the Canada Research Chairs Program, the Canada Foundation for Innovation and China Scholarship Council Fellowships (to Y.S. and R.Y.).

CONFLICT OF INTEREST

The authors declare no conflict of interest.

AUTHOR CONTRIBUTIONS

Yulin Sun, Ruonan Yao, Zhonghua Wang and Reinhard Jetter designed the experiments; Yulin Sun, Ruonan Yao, Xiufeng Ji, Hongqi Wu and Alvaro Luna acquired the data; Yulin Sun, Ruonan Yao and Reinhard Jetter analyzed the data; and Yulin Sun and Reinhard Jetter wrote the manuscript.

DATA AVAILABILITY STATEMENT

All relevant data can be found within the manuscript and its supporting materials.

SUPPORTING INFORMATION

Additional Supporting Information may be found in the online version of this article.

Figure S1. *ScARS* cloning, gene structure, protein hydrophobicity and sequence comparison with similar *S. cereale* proteins.

Figure S2. Identification of minor alkylresorcinolic compounds found in total lipid extracts of yeast expressing rye alkylresorcinol synthase, ScARS.

Figure S3. Sampling design employed to test spatial and temporal correlation between alkylresorcinol accumulation and ScARS gene expression within the second leaf (first true leaf) of rye.

Figure S4. Relative composition of wax mixtures along the second leaf of rye plants in four growth stages.

Figure S5. Phylogenetic relationship between ARSs and other related type-III PKSs (CHSs/CHSLs) in plants and bacteria.

Table S1. Primers used for RACE, cloning and qRT-PCR.

Table S2. Amino acid sequence identities between rye alkylresorcinol synthase, ScARS, and previously characterized grass ARSs as well as rye CHSs.

Table S3. Wax composition on the rye cv. Xiaoheimai penduncle, flag leaf blade, flag leaf sheath, stem and seedling leaf blade. Coverages are given in units of μg dm^{-2} as averages of four parallels plus/minus standard deviation.

Table S4. Wax composition on the rye cv. Xiaoheimai awn, glume seed coat and root. Coverages are given in units of μg g^{-1} DW as averages of four parallels plus/minus standard deviation.

Table S5. Chain length distribution of wax compounds with alkylresorcinol structures on the rye cv. Xiaoheimai penduncle, flag leaf blade, flag leaf sheath, stem and seedling leaf blade. Coverages are given in units of μg dm^{-2} as averages of four parallels plus/minus standard deviation.

Table S6. Chain length distribution of wax compounds with alkylresorcinol structures on the rye cv. Xiaoheimai awn, glume seed coat and root. Coverages are given in units of μg g^{-1} DW as averages of four parallels plus/minus standard deviation.

Table S7. Chain length distribution of wax compounds on the rye cv. Xiaoheimai peduncle, flag leaf blade, flag leaf sheath, stem and seedling leaf blade. Coverages are given in units of μg dm^{-2} as averages of four parallels plus/minus standard deviation.

Table S8. Chain length distribution of wax compounds on the rye cv. Xiaoheimai awn, glume seed coat and root. overages are given in units of μg g^{-1} DW as averages of four parallels plus/minus standard deviation.

Table S9. Accession numbers of genes used in this work.

REFERENCES

Abbadi, A., Domergue, F., Bauer, J., Napier, J.A., Welti, R., Zähringer, U., Cirpus, P. and Heinz, E. (2004) Biosynthesis of very-long-chain polyunsaturated fatty acids in transgenic oilseeds: constraints on their accumulation. *Plant Cell*, **16**, 2734–2748.

Abe, I. and Morita, H. (2010) Structure and function of the chalcone synthase superfamily of plant type III polyketide synthases. *Nat. Prod. Rep.* **27**, 809–838.

Adamski, N.M., Bush, M.S., Simmonds, J., Turner, A.S., Mugford, S.G., Jones, A., Findlay, K., Pedentchouk, N., von Wettstein-Knowles, P. and Uauy, C. (2013) The *Inhibitor of wax 1* locus (*Iw1*) prevents formation of β- and OH-β-diketones in wheat cuticular waxes and maps to a sub-cM interval on chromosome arm 2BS. *Plant J.* **74**, 989–1002.

Andersson, A.A.M., Kamal-Eldin, A., Fraś, A., Boros, D. and Åman, P. (2008) Alkylresorcinols in wheat varieties in the HEALTHGRAIN diversity screen. *J. Agric. Food Chem.* **56**, 9722–9725.

© 2020 The Authors.
The Plant Journal © 2020 John Wiley & Sons Ltd,

Austin, M.B. and Noel, J.P. (2003) The chalcone synthase superfamily of type III polyketide synthases. *Nat. Prod. Rep.* **20**, 79–110.

Austin, M.B., Bowman, M.E., Ferrer, J.-L., Schröder, J. and Noel, J.P. (2004) An aldol switch discovered in stilbene synthases mediates cyclization specificity of type III polyketide synthases. *Chem. Biol.* **11**, 1179–1194.

Bach, L., Michaelson, L.V., Haslam, R. *et al.* (2008) The very-long-chain hydroxy fatty acyl-CoA dehydratase PASTICCINO2 is essential and limiting for plant development. *Proc. Natl Acad. Sci. USA*, **105**, 14 727–14 731.

Barr, J.R., Murty, V., Yamaguchi, K., Singh, S., Smith, D.H. and Hecht, S.M. (1988) 5-Alkylresorcinols from *Hakea amplexicaulis* that cleave DNA. *Chem. Res. Toxicol.* **1**, 204–207.

Bauer, E., Schmutzer, T., Barilar, I. *et al.* (2017) Towards a whole-genome sequence for rye (*Secale cereale* L.). *Plant J.* **89**, 853–869.

Bernard, A. and Joubes, J. (2013) Arabidopsis cuticular waxes: Advances in synthesis, export and regulation. *Prog. Lipid Res.* **52**, 110–129.

Bernard, A., Domergue, F., Pascal, S., Jetter, R., Renne, C., Faure, J.D., Haslam, R.P., Napier, J.A., Lessire, R. and Joubes, J. (2012) Reconstitution of plant alkane biosynthesis in yeast demonstrates that Arabidopsis ECERIFERUM1 and ECERIFERUM3 are core components of a very-long-chain alkane synthesis complex. *Plant Cell*, **24**, 3106–3118.

Busta, L. and Jetter, R. (2018) Moving beyond the ubiquitous: the diversity and biosynthesis of specialty compounds in plant cuticular waxes. *Phytochem. Rev.* **17**, 1275–1304.

Cook, D., Rimando, A.M., Clemente, T.E. *et al.* (2010) Alkylresorcinol synthases expressed in *Sorghum bicolor* root hairs play an essential role in the biosynthesis of the allelopathic benzoquinone sorgoleone. *Plant Cell*, **22**, 867–887.

Cserzö, M., Wallin, E., Simon, I., Von Heijne, G. and Elofsson, A. (1997) Prediction of transmembrane α-helices in prokaryotic membrane proteins: the dense alignment surface method. *Protein Eng.* **10**, 673–676.

Deszcz, L. and Kozubek, A. (2000) Higher cardol homologs (5-alkylresorcinols) in rye seedlings. *Biochim. Biophys. Acta*, **1483**, 241–250.

Dörmann, P., Voelker, T.A. and Ohlrogge, J.B. (2000) Accumulation of palmitate in Arabidopsis mediated by the acyl-acyl carrier protein thioesterase FATB1. *Plant Physiol.* **123**, 637–643.

Dring, J.V., Kite, G.C., Nash, R.J. and Reynolds, T. (1995) Chemicals in aroids: a survey, including new results for polyhydroxy alkaloids and alkylresorcinols. *Bot. J. Linn. Soc.* **117**, 1–12.

Edgar, R.C. (2004) MUSCLE: multiple sequence alignment with high accuracy and high throughput. *Nucleic Acids Res.* **32**, 1792–1797.

Færgeman, N.J., Black, P.N., Zhao, X.D., Knudsen, J. and DiRusso, C.C. (2001) The acyl-CoA synthetases encoded within *FAA1* and *FAA4* in *Saccharomyces cerevisiae* function as components of the fatty acid transport system linking import, activation, and intracellular utilization. *J. Biol. Chem.* **276**, 37 051–37 059.

Fich, E.A., Segerson, N.A. and Rose, J.K. (2016) The plant polyester cutin: biosynthesis, structure, and biological roles. *Annu. Rev. Plant Biol.* **67**, 207–233.

Funa, N., Ozawa, H., Hirata, A. and Horinouchi, S. (2006) Phenolic lipid synthesis by type III polyketide synthases is essential for cyst formation in *Azotobacter vinelandii*. *Proc. Natl Acad. Sci. USA*, **103**, 6356–6361.

Funa, N., Awakawa, T. and Horinouchi, S. (2007) Pentaketide resorcylic acid synthesis by type III polyketide synthase from *Neurospora crassa*. *J. Biol. Chem.* **282**, 14 476–14 481.

Gagne, S.J., Stout, J.M., Liu, E.W., Boubakir, Z., Clark, S.M. and Page, J.E. (2012) Identification of olivetolic acid cyclase from *Cannabis sativa* reveals a unique catalytic route to plant polyketides. *Proc. Natl Acad. Sci. USA*, **109**, 12 811–12 816.

García, S., García, C., Heinzen, H. and Moyna, P. (1997) Chemical basis of the resistance of barley seeds to pathogenic fungi. *Phytochemistry*, **44**, 415–418.

Gietz, R.D. and Woods, R.A. (2002) Transformation of yeast by lithium acetate/single-stranded carrier DNA/polyethylene glycol method. In *Methods in Enzymology* (Guthrie, C. and Fink, G.R. eds). New York, NY: Academic Press, pp. 87–96.

Gülz, P.-G., Müller, E., Schmitz, K., Marner, F.-J. and Güth, S. (1992) Chemical composition and surface structures of epicuticular leaf waxes of *Ginkgo biloba*, *Magnolia grandiflora* and *Liriodendron tulipifera*. *Z. Nat. C*, **47**, 516–526.

Haslam, T.M. and Kunst, L. (2013) Extending the story of very-long-chain fatty acid elongation. *Plant Sci.* **210**, 93–107.

Hegebarth, D. and Jetter, R. (2017) Cuticular waxes of *Arabidopsis thaliana* shoots: cell-type-specific composition and biosynthesis. *Plants*, **6**, 27.

Hegebarth, D., Buschhaus, C., Joubès, J., Thoraval, D., Bird, D. and Jetter, R. (2017) Arabidopsis ketoacyl-CoA synthase 16 (KCS16) forms C_{36}/C_{38} acyl precursors for leaf trichome and pavement surface wax. *Plant Cell Environ.* **40**, 1761–1776.

Jetter, R. and Schäffer, S. (2001) Chemical composition of the *Prunus laurocerasus* leaf surface. Dynamic changes of the epicuticular wax film during leaf development. *Plant Physiol.* **126**, 1725–1737.

Jetter, R., Klinger, A. and Schäffer, S. (2002) Very long-chain phenylpropyl and phenylbutyl esters from *Taxus baccata* needle cuticular waxes. *Phytochemistry*, **61**, 579–587.

Jetter, R., Kunst, L. and Samuels, A.L. (2007) Composition of plant cuticular waxes. In *Biology of the Plant Cuticle* (Riederer, M. and Muller, C. eds). Oxford: Blackwell, pp. 145–181.

Ji, X. and Jetter, R. (2008) Very long chain alkylresorcinols accumulate in the intracuticular wax of rye (*Secale cereale* L.) leaves near the tissue surface. *Phytochemistry*, **69**, 1197–1207.

Kienzle, S., Carle, R., Sruamsiri, P., Tosta, C. and Neidhart, S. (2013) Occurrence of alk (en) ylresorcinols in the fruits of two mango (*Mangifera indica* L.) cultivars during on-tree maturation and postharvest storage. *J. Agric. Food Chem.* **62**, 28–40.

Kim, S.Y., Colpitts, C.C., Wiedemann, G. *et al.* (2013) *Physcomitrella* PpORS, basal to plant type III polyketide synthases in phylogenetic trees, is a very long chain 2′-oxoalkylresorcinol synthase. *J. Biol. Chem.* **288**, 2767–2777.

Kulawinek, M. and Kozubek, A. (2008) Quantitative determination of alkylresorcinols in cereal grains: independence of the length of the aliphatic side chain. *J. Food Lipids*, **15**, 251–262.

Lai, C., Kunst, L. and Jetter, R. (2007) Composition of alkyl esters in the cuticular wax on inflorescence stems of *Arabidopsis thaliana cer* mutants. *Plant J.* **50**, 189–196.

Landberg, R., Kamal-Eldin, A., Salmenkallio-Marttila, M., Rouau, X. and Åman, P. (2008) Localization of alkylresorcinols in wheat, rye and barley kernels. *J. Cereal Sci.* **48**, 401–406.

Larson, T.R. and Graham, I.A. (2001) Technical advance: a novel technique for the sensitive quantification of acyl CoA esters from plant tissues. *Plant J.* **25**, 115–125.

Li, L., Aslam, M., Rabbi, F., Vanderwel, M.C., Ashton, N.W. and Suh, D.-Y. (2018) PpORS, an ancient type III polyketide synthase, is required for integrity of leaf cuticle and resistance to dehydration in the moss, *Physcomitrella patens*. *Planta*, **247**, 527–541.

Li-Beisson, Y., Shorrosh, B., Beisson, F., Andersson, M.X., Arondel, V., Bates, P.D., Baud, S., Bird, D., DeBono, A. and Durrett, T.P. (2013) Acyl-lipid metabolism. *Arabidopsis Book*, **11**, e0161.

Livak, K.J. and Schmittgen, T.D. (2001) Analysis of relative gene expression data using real-time quantitative PCR and the $2^{-\Delta\Delta C}$T method. *Methods*, **25**, 402–408.

Magnucka, E.G., Suzuki, Y., Pietr, S.J., Kozubek, A. and Zarnowski, R. (2007) Action of benzimidazole fungicides on resorcinolic lipid metabolism in rye seedlings depends on thermal and light growth conditions. *Pestic. Biochem. Physiol.* **88**, 219–225.

Matsuzawa, M., Katsuyama, Y., Funa, N. and Horinouchi, S. (2010) Alkylresorcylic acid synthesis by type III polyketide synthases from rice *Oryza sativa*. *Phytochemistry*, **71**, 1059–1067.

Oh, C.-S., Toke, D.A., Mandala, S. and Martin, C.E. (1997) *ELO2* and *ELO3*, homologues of the *Saccharomyces cerevisiae ELO1* gene, function in fatty acid elongation and are required for sphingolipid formation. *J. Biol. Chem.* **272**, 17 376–17 384.

Racovita, R.C., Hen-Avivi, S., Fernandez-Moreno, J.-P., Granell, A., Aharoni, A. and Jetter, R. (2016) Composition of cuticular waxes coating flag leaf blades and peduncles of *Triticum aestivum* cv. Bethlehem. *Phytochemistry*, **130**, 182–192.

Richardson, A., Franke, R., Kerstiens, G., Jarvis, M., Schreiber, L. and Fricke, W. (2005) Cuticular wax deposition in growing barley (*Hordeum vulgare*) leaves commences in relation to the point of emergence of epidermal cells from the sheaths of older leaves. *Planta*, **222**, 472–483.

Riederer, M. and Müller, C. (2007) *Biology of the Plant Cuticle*. Oxford: Blackwell.

Ross, A.B., Kamal-Eldin, A., Jung, C., Shepherd, M.J. and Åman, P. (2001) Gas chromatographic analysis of alkylresorcinols in rye (*Secale cereale* L) grains. *J. Sci. Food Agric.* **81**, 1405–1411.

© 2020 The Authors.

Ross, A.B., Shepherd, M.J., Schüpphaus, M., Sinclair, V., Alfaro, B., Kamal-Eldin, A. and Åman, P. (2003) Alkylresorcinols in cereals and cereal products. *J. Agric. Food Chem.* **51**, 4111–4118.

Rowland, O., Zheng, H.Q., Hepworth, S.R., Lam, P., Jetter, R. and Kunst, L. (2006) *CER4* encodes an alcohol-forming fatty acyl-coenzyme A reductase involved in cuticular wax production in Arabidopsis. *Plant Physiol.* **142**, 866–877.

Samuels, L., Kunst, L. and Jetter, R. (2008) Sealing plant surfaces: Cuticular wax formation by epidermal cells. *Annu. Rev. Plant Biol.* **59**, 683–707.

Seitz, L.M. (1992) Identification of 5-(2-oxoalkyl)resorcinols and 5-(2-oxoalkenyl)resorcinols in wheat and rye grains. *J. Agric. Food Chem.* **40**, 1541–1546.

Sparkes, I.A., Runions, J., Kearns, A. and Hawes, C. (2006) Rapid, transient expression of fluorescent fusion proteins in tobacco plants and generation of stably transformed plants. *Nat. Protoc.* **1**, 2019–2025.

Stymne, S. and Stobart, A.K. (1984) Evidence for the reversibility of the acyl-CoA:lysophosphatidylcholine acyltransferase in microsomal preparations from developing safflower (*Carthamus tinctorius* L.) cotyledons and rat liver. *Biochem. J.* **223**, 305–314.

Stymne, S., Stobart, A.K. and Glad, G. (1983) The role of the acyl-CoA pool in the synthesis of polyunsaturated 18-carbon fatty acids and triacylglycerol production in the microsomes of developing safflower seeds. *Biochim. Biophys. Acta*, **752**, 198–208.

Suh, M.C., Samuels, A.L., Jetter, R., Kunst, L., Pollard, M., Ohlrogge, J. and Beisson, F. (2005) Cuticular lipid composition, surface structure, and gene expression in Arabidopsis stem epidermis. *Plant Physiol.* **139**, 1649–1665.

Suzuki, Y., Saitoh, C., Hyakutake, H., Kono, Y. and Sakurai, A. (1996) Specific accumulation of antifungal 5-Alk(en)ylresorchinol homologs in etiolated rice seedlings. *Biosci. Biotechnol. Biochem.* **60**, 1786–1789.

Suzuki, Y., Esumi, Y. and Yamaguchi, I. (1999) Structures of 5-alkylresorcinol-related analogues in rye. *Phytochemistry*, **52**, 281–289.

Tribouillois, H., Fort, F., Cruz, P., Charles, R., Flores, O., Garnier, E. and Justes, E. (2015) A functional characterisation of a wide range of cover crop species: growth and nitrogen acquisition rates, leaf traits and ecological strategies. *PLoS One*, **10**, e0122156–e0122156.

Wang, J., Gao, X. and Wang, Z. (2019) Non-destructive determination of alkylresorcinol (ARs) content on wheat weed surfaces and prediction of ARs content in whole-grain flour. *Molecules*, **24**, 1329.

Yeats, T.H. and Rose, J.K.C. (2013) The formation and function of plant cuticles. *Plant Physiol.* **163**, 5–20.

Żarnowska, E.D., Żarnowski, R. and Kozubek, A. (2000) Alkylresorcinols in fruit pulp and leaves of *Ginkgo biloba* L. *Z. Nat. C* **55**, 881–885.

Zarnowski, R. and Kozubek, A. (1999) Alkylresorcinol homologs in *Pisum sativum* L. varieties. *Z. Nat. C* **54**, 44–48.

Zarnowski, R. and Suzuki, Y. (2004) 5-n-Alkylresorcinols from grains of winter barley (*Hordeum vulgare* L.). *Z. Nat. C* **59**, 315–317.

© 2020 The Authors.
The Plant Journal © 2020 John Wiley & Sons Ltd,